THESIS

USING CANNABIDIOL AND TRAZODONE TO TREAT PROTEIN MISFOLDING NEURODEGENERATIVE DISEASE IN *C. ELEGANS*

Submitted by

Vincenzo S. Gilberto

Department of Environmental and Radiological Health Sciences

In partial fulfillment of requirements

For the Degree of Master of Science

Colorado State University

Fort Collins, Colorado

Summer 2022

Master's Committee:

Advisor: Julie A. Moreno

Marie Legare
Stephanie McGrath
Katriana Popichak
Gregory Dooley

ABSTRACT

USING CANNABIDIOL AND TRAZODONE TO TREAT PROTEIN MISFOLDING NEURODEGENERATIVE DISEASE IN *C. ELEGANS*

Alzheimer's disease is one of the most common neurodegenerative disorders and is typically characterized by the accumulation of the misfolded proteins Amyloid-Beta ($A\beta_{1-42}$) and/or hyperphosphorylation of Tau (p-Tau). Despite the lack of a cure for the disease, it is well known that targeting signaling pathways involved in reactive oxygen species (ROS) or the unfolded protein response (UPR) mitigates the toxic effects of misfolded proteins, including behavioral deficits, glial inflammation, and neuronal toxicity. Laboratory animals, which have long been used to study this disease, have been genetically modified to express the two aforementioned proteins and express similar deleterious effects. However, despite the individual targeting of these pathways—although neuroprotective for some time—the laboratory model still succumbs to the disease. In this work, we hypothesized that drug-stacking Cannabidiol and Trazadone, which respectively target ROS production and UPR, would improve the neuronal function and extend the lifespan of neurodegenerative nematode models. To test this hypothesis, we utilized specific strains of *C. elegans* that have been genetically modified to contain the two common misfolded proteins found to aggregate in the brains of patients with Alzheimer's, $A\beta_{1-42}$ and p-Tau. The AD-modeled nematodes were designed to parallel the middle- and late-stage in humans, starting at the point where signs of the disease first begin to become apparent. This research used Cannabidiol and Trazodone to inhibit ROS and UPR, respectively. Our experiments revealed that neurodegenerative *C. elegans* motility and lifespan significantly

improved with both combination and isolated treatments of CBD and TRA. Our data also suggest that genetically susceptible neurodegenerative *C. elegans* can benefit from both full-life and late-stage rescue utilizing CBD and TRA. We predict these results may help guide future experimentation that incorporates the use of both CBD and TRA in higher organisms, including rodent models of neurodegeneration and aged canines with cognitive decline.

Keywords: Alzheimer's disease, *C. elegans*, cannabidiol, trazodone, protein misfolding, hyperphosphorylation of Tau (p-Tau), Amyloid-Beta ($A\beta_{1-42}$)

ACKNOWLEDGMENTS

My scientific endeavor has had many ups and downs; completing this thesis and successfully defending was a team effort. I would like to thank Dr. Stephanie McGrath for introducing the idea of using Cannabidiol and all her hard work showing the PK/PD values in her previous canine publications. I would like to thank Dr. Katriana Popichak for all her help troubleshooting the immunofluorescence work and giving valuable input on stains to use. I would like to thank Dr. Greg Dooley for his expertise and guidance using the LC-MS/MS. I would like to thank Dr. Marie Legare for overviewing my data and overall work, guiding me on how to be a better scientist. Finally, I would like to acknowledge Dr. Julie Moreno for spearheading this project and mentoring both the big picture and nitty gritty details of what it takes and means to be a scientist.

DEDICATION

In loving memory, I want to dedicate this project to Dr. William Hanneman — "H." I had the pleasure of meeting H. through martial arts at age 20. It is strange to state this now because it seems as if I knew him so much longer than only 3 years. He was always a pillar of strength and someone to look up to and emulate. He took the position of a father figure in my life due to my own father's diagnosis of Alzheimer's disease, which quickly took any normalcy of a father-son bond with my dad. H. was always there for mentorship regarding classwork, lab work, and Brazilian Jiu-Jitsu help. Most importantly, H. mentored me to be a better man in a period when I wanted to give up on schooling because of my father's quickly developing symptoms. You will never be forgotten and will always be loved, H.

TABLE OF CONTENTS

LIST OF FIGURES

CHAPTER 1

INTRODUCTION

1.1 Background on Alzheimer's Disease

Alzheimer's disease (AD) has become one of the most prevalent neurodegenerative disorders. According to the Centers for Disease Control and Prevention (CDC; 2020), millions of Americans live with AD and its debilitating consequences, which most notably include cognitive impairment, loss of mobility, and shortened lifespan. However, AD is a disease of unknown origins; the CDC states that, "In 2020, an estimated 5.8 million Americans aged 65 years or older had Alzheimer's disease. This number is projected to nearly triple to 14 million people by 2060" (Centers for Disease Control and Prevention [CDC], 2020, para. 2). The rise in prevalence of this disease relates to the overall increased lifespan of humans due to advances in medicine. Research regarding better understanding of AD has included—but is not limited to—environmental factors, gene polymorphisms, and the gut-brain access. One aspect of AD researchers have agreed upon are its pathological hallmarks, which are: the presence of misfolded proteins Amyloid-Beta (1–42) ($A\beta_{1\text{-}42)}$ and hyperphosphorylated Tau (p-Tau), which are uniquely present in the entorhinal cortex and hippocampal regions of the brain (Bloom, 2014).

1.2 Current Treatment Options

Despite our understanding of the pathogenesis of AD, both clinically and microscopically, a cure is yet to be identified. The medications prescribed by physicians do not target these cellular dysfunctions but rather circumvent clinical symptoms or neuronal transmissions. An example of this is donepezil (Aricept®), which is the most widely prescribed medication to combat the disease. The drug acts as an acetylcholine (ACh) antagonist and it is

hypothesized that treating AD patients with this medication results in making the neurotransmitter ACh more bioavailable (Birks & Harvey, 2018). Specifically, the medication allows for the increased transmission of acetylcholine to be more readily available throughout the body and subsequently increase neuronal function. However, due to this mechanism of action (MOA), donepezil has a narrow therapeutic range. Moreover, while this can improve symptoms of AD patients, it should be noted that excess ACh has been associated with GI issues. Doses of 5 mg increasing to 10 mg are considered optimal for patients with mild to moderate AD; for those with moderate to severe AD, the suggested dosage is 10 mg up to 23 mg (Kumar et al., 2021). Any increase in the dosage must be undertaken with careful consideration (Cummings et al., 2013). Donepezil does not target the hallmarks of AD, including the misfolding of proteins or the free radicals produced by misfolded proteins. Given these two facts, patients with AD taking this medication may experience some relief of clinical symptoms but will eventually reach a threshold where the medication becomes ineffective due to the presence of misfolded proteins.

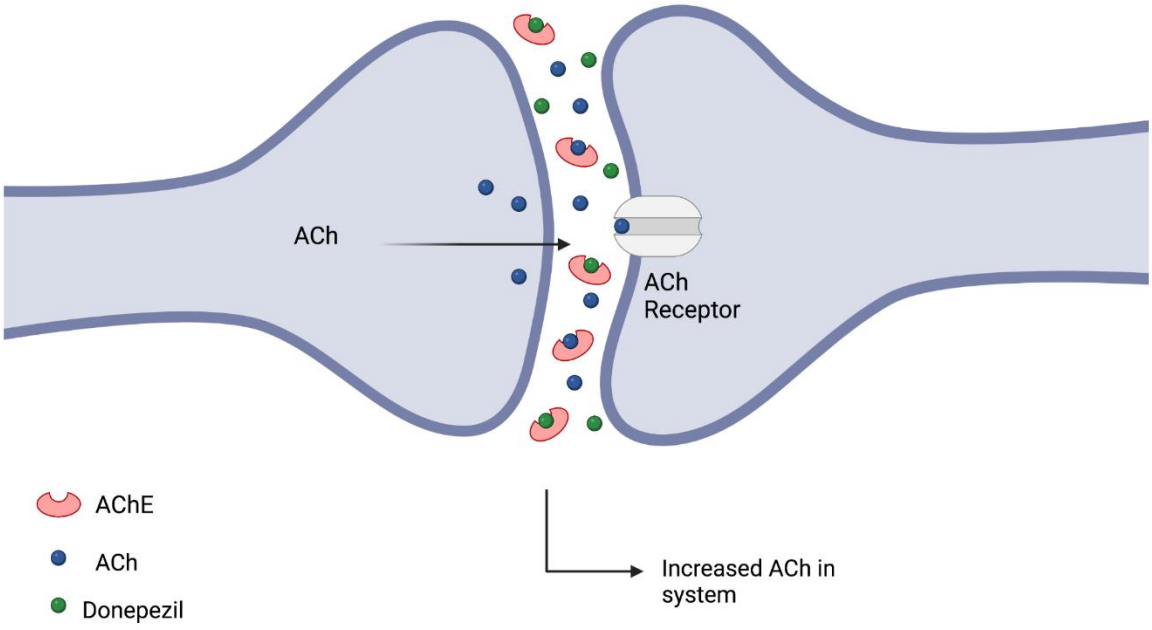

Figure 1.1. *Schematic Diagram Depicting Mechanism of Action of Donepezil*

Note: Donepezil treatment allows excess ACh to accumulate in the synaptic cleft increasing neuronal transmission. Figure developed using information from Birks and Harvey (2018), Colovic et al. (2013), and Lee et al. (2015). Image created by author using BioRender.

While donepezil does not explicitly target misfolded proteins $A\beta_{1\text{-}42}$ and p-Tau, newer drugs have made their way into the market that do (Goodwin, 2021). One such medication is aducanumab (Aduhelm®), an FDA-approved monoclonal antibody treatment that targets $A\beta_{1\text{-}42}$ specifically ("Aducanumab (Aduhelm) for Alzheimer's disease," 2021). While targeting the misfolded proteins seems to be a more promising route, multiple controversies surround aducanumab. The first of which to address is that the treatment's original cost was $56,000 but due to this astronomical price, Medicare stepped in and limited the cost to $28,000, which will still prevent many of those in need of it from having access (Alonso-Zaldivar, 2022). More importantly, however, the bulk of the controversy stems from the fact that the drug underwent the U.S. Food and Drug Administration's (FDA) Accelerated Approval Pathway. Despite its inability to sufficiently meet the FDA's effectiveness guidelines to show significance in clinical trials, it was nonetheless fast-tracked to the market (Sutton, 2022). This executive decision was primarily due to the lack of novel treatments for AD.

1.3 Statement of the Problem

The medications currently available mainly work to address existing $A\beta_{1\text{-}42}$ plaques and ACh ("Aducanumab (Aduhelm) for Alzheimer's disease," 2021; Birks & Harvey, 2018). There has yet to be a medication that specifically and successfully targets the plaque formation or the cellular stress produced by the accumulation of these misfolded proteins. In this research, the specific targets are cellular stress pathways responsible for the generation of reactive oxygen species (ROS) and repairing misfolded proteins, as we believe that cotreatment with stacking chemically unique drugs that individually address a variety of cellular stress avenues is a promising avenue of AD treatment.

CHAPTER 2

LITERATURE REVIEW

2.1 The Unfolded Protein Response

Understanding how the accumulation of misfolded proteins occurs and the way these misfolded proteins behave is critical to the development of treatment plans and the understanding of the mechanisms behind the disease's progression. Proteins have specific conformations that allow them to perform homeostatic functions. Proteins can be misfolded, which most often involves deviating from standard alpha-helix (α-helix) configuration to one of beta-sheet (β-sheets), which is not always deleterious, but when occurring in the 1-42 configuration is damaging to the body (Gross, 2000). Protein misfolding is a result of both a malfunction in a cell's failsafe mechanisms as well as in its adhering to proper energy minimization pathways during folding. Typically, when proteins are misfolded, specific cellular translational control pathways—such as the unfolded protein response (UPR) and protein chaperones—attempt to correct these misfolded proteins by either correctly refolding them or degrading them. However, due to the exponential nature of AD and the overall typical degradation of cells in an aging organism, these misfolded proteins in a sense circumvent these safety mechanisms and are thereby able to accumulate, wreaking havoc on the neurological function of the organism (Clark, 2004; Reynaud, 2010; Zheng et al., 2013). Understanding how AD progresses and addressing the avenues taken by misfolded proteins earlier could hinder the exponential progression of the disease.

The UPR pathway is the body's primary cellular response to misfolded proteins for both repair or degradation (see Fig. 2.1). Endoplasmic reticulum (ER) stress response genes work by

addressing misfolded proteins by either clearing them from the cell or properly refolding them to perform their homeostatic functions (Simmons et al., 2009). During events of ER stress induced by misfolded proteins, the main activated pathway is the PERK pathway. Downstream of PERK is the eIF2α, which, when functioning correctly, will address these misfolded proteins by degrading them. However, in the event of chronic ER stress, the eIF2α pathway will phosphorylate (p-eIF2α), effectively shutting down the pathway's essential functions (Halliday et al., 2017; Moreno et al., 2013; Radford et al., 2015). It has previously been found that the cognition of Alzheimer's-modeled organisms improved when compounds that target the PERK pathway were used (Halliday et al., 2017; Moreno et al., 2013).

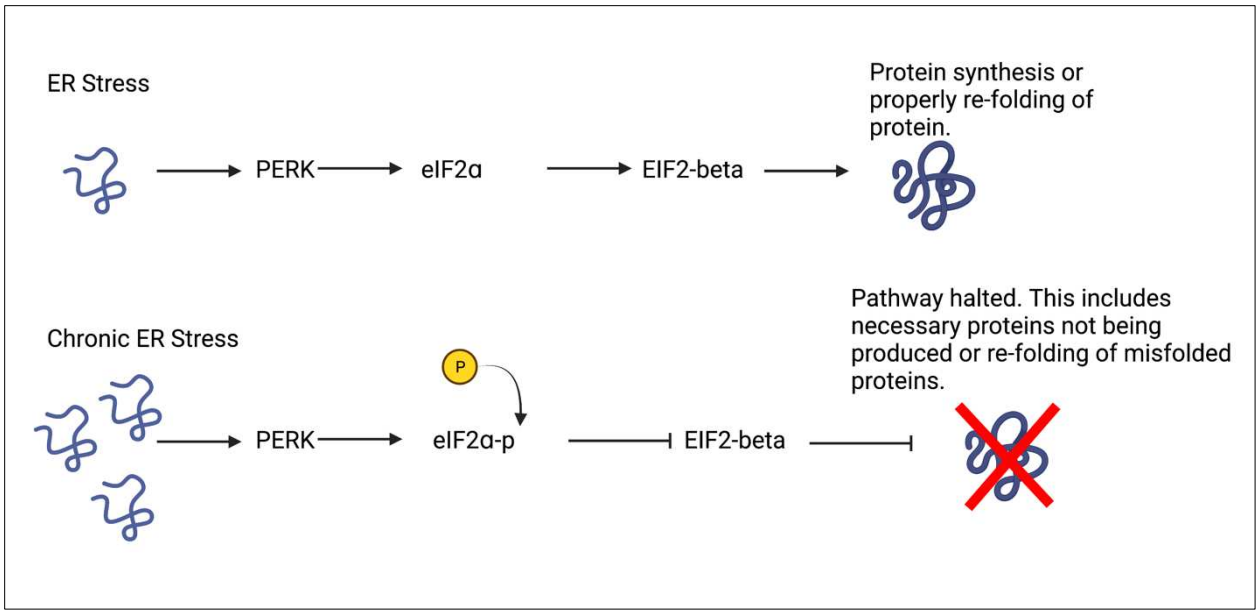

Figure 2.1. *Schematic Diagram Depicting UPR Pathway Under ER Stress*

Note. A general outline of the pathway's response under both normal conditions and chronic stress in the presence of misfolded proteins. Image created by author using BioRender.

2.2 Reactive Oxygen Species in the AD Model

The second major consideration identified after the UPR pathway is the oxidative stress cellular response pathway, which was examined due to its ability to address the reactive oxygen species (ROS) produced by misfolded proteins. During chronic exposure to A$\beta_{1\text{-}42}$ and p-Tau, elevated levels of ROS induce the transduction of Nuclear factor erythroid-2 related factor 2 (Nrf-2) to act on the antioxidant response element (ARE) and activate downstream gene expression, which scavenges for ROS to detoxify the cell (Simmons et al., 2009; Sotolongo et al., 2020).

2.3 *C. elegans* as Model Organism

The model organism identified for use in the current study was *Caenorhabditis elegans* (*C. elegans*), a microscopic nematode that has been used as a biological model organism dating

back to the 1960s (Brenner, 1974). *C. elegans* possesses numerous aspects that makes it ideal for investigations, especially in the laboratory modeling of AD. First of all, it has a shorter lifespan compared to those of more traditional model organisms (e.g., mice or rats), with the Wild Type (N2) on average having a lifespan of less than 35 days (Urban et al., 2021). Moreover, nematodes are relatively cheap and, due to being hermaphroditic, can progenerate offspring by themselves. *C. elegans* then can be transferred to agar-rich plates and give rise to plates full of nematodes of the same genetic background.

CHAPTER 3

METHODS AND MATERIALS

This chapter will review the materials and methods used in the experiments. The maintenance of the nematodes and the buffers utilized throughout will also be described. Finally, the methods used to collect and analyze the data will be discussed.

3.1 Development of Treatment Plan

Despite the many advances and discoveries in the area of therapeutics, certain factors either have not been addressed or have been altogether disregarded. In an effort to address those gaps while taking a practical approach to our methodology, a list of significant considerations was developed through the literature review presented in Chapter 2. The first major consideration was the type of drugs to be examined in the treatments utilized in the study. Specifically, the goal was to recruit two existing, inexpensive, and previously FDA-approved pharmaceutical compounds for a drug-stacking therapy treatment with the aim being drug re-purposing and an affordable alternative to costly existing products (e.g., aducanumab). This was done to address the previously-discussed drawbacks to the mechanisms of action that have been found to target the UPR and ROS cellular pathways (Chaudhuri & Paul, 2006; Halliday et al., 2017; Zhang et al., 2022).

3.1.1 Compounds

To address ROS, the compound of interest selected for this pathway had to have a wide therapeutic range to allow for increasing doses due to the exponential increase of misfolded proteins characteristic of AD. Targeting this separate pathway in tandem with a known UPR-targeting compound of interest introduces a unique approach compared to the two previously-

mentioned approved treatments of antibody treatment and increasing ACh. After making the case for choosing the drugs of interest it was then necessary to establish both a model organism and an approach to deduce the timing/dosing required to significantly improve the selected model organism's lifespan with neurodegenerative disease.

3.1.2 Model Organism

Nematodes for this research were obtained from the Caenorhabditis Genetics Center (CGC), which has a comprehensive library of nematodes with various genetic backgrounds and mutations. This study utilized four genetically different *C. elegans*. Two strains were assigned to each model, to act as an experimental and a control organism for each. The first model, the Aβ_{1-42}, consists of the GRU101 (Anti-Aβ Aggr.) and GRU102 (Pro-Aβ Aggr.) strains. The Anti-Aβ Aggr. strain genotype is almost identical to the Wild Type, excluding two fluorescent protein markers (Fong et al., 2016). The experimental strain was genetically modified to express the misfolded protein via transfection of human minigene to express Aβ_{1-42} in the neurons (Fong et al., 2016).

The engineers of the strain were able to categorize the nematodes' age and the progression of protein accumulation in the AD-model organism, which has an average lifespan of 30 days. The researchers utilized both behavioral assays and western blots to deduce that the nematodes would be at middle-age on Day 8 and that Aβ_{1-42} peaked on Day 12, making them at that point senior nematodes with the overall decreased motility correlating with neuronal dysfunction (Fong et al., 2016). This established the roadmap regarding the expected time of neuronal damage and the period where treatments would be implemented.

The p-Tau model, like the Aβ_{1-42} model, contains a control organism (that does not express the Tau protein) and an experimental organism (that does express p-Tau). The control

strain BR6427 (Anti-Tau Aggr.) has been modified through double-crossing strains. This crossing of strains results in an organism with the inability to form Tau proteins (Fatouros et al., 2012). The experimental strain BR5706 (Pro-Tau Aggr.) was also created by crossing two separate strains of *C. elegans*. Unlike its control, the Pro-Tau Aggr. strain expresses aggregation of p-Tau protein conferring into p-Tau in the GABAergic motor neurons. For both experimental strains, locomotion, lifespan, and neuronal integrity were severely affected. This manifested as diminished synaptic function resulting in worse motility and a shortened lifespan (Fatouros et al., 2012). Unlike in previous research, the engineers of the Tauopathy model did not include a mapped lifespan of the formation of p-Tau. However, the observations regarding the lifespan of $A\beta_{1\text{-}42}$ were applied to the Tauopathy model and the Pro-Tau Aggr. was treated at the same time points.

3.2 Hypothesis of Treatment Plan

The investigation required that a dosing schedule be established that could ideally be translational to humans; therefore, the nematodes were dosed with the drug-stacking regimen for full-life, middle-age, and slightly past the senior mark. Since current treatment options for AD are limited and do not seem to address the toxicity of misfolded proteins, the nematodes were treated with the drugs of interest over the similar stages of life during which most patients with AD would be diagnosed with the disease. This was done with the aim of obtaining insights into how to ameliorate the pathogenesis of the disease and extend lifespan. *C. elegans* also has a unique morphology that consists of glial cells comprising a nerve ring, which is representative of the blood brain barrier (BBB) in humans (Oikonomou & Shaham, 2011). It was essential that the drugs we investigated could cross the BBB of both humans and the equivalent in *C. elegans* to strengthen the application of the study data for future translational research.

3.3 Drugs of Interest

3.3.1 Cannabidiol

The first drug of interest (DOI) investigated was Cannabidiol (CBD), which is a phytochemical that derives from the *Cannabis sativa* family of plants. The metabolism of CBD is largely associated with the endocannabinoid receptors 2-AG and *N*-arachidonoyl-ethanolamine (anandamide/AEA). These have been identified in nearly all mammals, including *C. elegans* (Land et al., 2021). CBD binds to AEA and independently undergoes phase II transformation via N-acyltransferase and subsequently undergoes N-acyl-phosphatidylethanolamine acting as a cannabinoid receptor type 1 (CB1) partial agonist (Maccarrone, 2017). However, when CBD interacts with endocannabinoid endogenous receptor 2-AG, it acts as an allosteric modulator for CB1 in the presence of Cannabidiol within *C. elegans* elucidating the beneficial effects by activating CB1 (Bakas et al., 2017). *C. elegans* when treated with CBD have increased longevity and higher heat stress tolerance over a wide range of dosages (0.4 mM to 4.0 mM; Land et al., 2021). Additionally, when *C. elegans* models of Alzheimer's disease are treated with CBD ameliorated the disease by acting as an ROS scavenger. These previously noted beneficial effects of CBD in nematode models are likely due to the binding of the endocannabinoid receptors 2-AG and AEA and the downstream activation of the CB1 receptor, making CBD an ideal compound to investigate for our models (Bisogno et al., 2001; Land et al., 2021; Ryberg et al., 2007).

Given that the UPR pathway is one of the primary mechanisms responsible for dealing with misfolded proteins, examination of CBD's potential action on the UPR was also of interest in this study. As previously discussed in Section 2.1, during ER stress the PERK pathway is activated by the dimerization and phosphorylation of PERK in the presence of aggregates or

misfolded proteins; the downstream consequences of chronic phosphorylation inhibits eIF2-α-p, which shuts down protein synthesis (Halliday et al., 2017). There is some evidence that suggests CBD acts on this pathway. In cell culture exposed to LPS, researchers found activation of phosphorylation of the eIF2-α pathway (Mecha et al., 2012). When a cultured cell is first exposed to LPS and subsequently treated with CBD, the overall phosphorylation of the eIF2-α decreases (Melas et al., 2018). While this is not the main reason for the utilization of CBD in this study, it could prove that treatments of neurodegenerative models with CBD and TRA may have a synergistic or additive effect on this pathway. However, the limited publications to date that have investigated *C. elegans* treated with CBD and its ability to be metabolized have at minimum established the organism's affinity for the drug in a diseased state.

As has been previously highlighted, *C. elegans* has an affinity and established pharmacokinetic response to CBD, which led to the next question posed in this study: What are the relative therapeutic and toxicological doses? Past research also has found that CBD is non-toxic and improves the overall quality of life of nematodes at doses between 10 µM–100 µM (Land et al., 2021). Moreover, *C. elegans* LD_{50} values have in the past been used as predicative of LD_{50} values for higher organisms (Hunt, 2017). One method used by researchers to assess CBD toxicity in *C. elegans* was by exposing the nematodes to heat stress. The researchers noted that 0.4 µM–4000 µM CBD was not toxic, and 40 µM was the most beneficial for heat stress survival (Land et al., 2021). Given the findings of these previous publications regarding CBD and its effects in nematodes, we treated our Alzheimer's model organism with doses ranging from 5 µM–40 µM. While the mechanisms have been cited, CBD's action on oxidative stress is not fully understood, and the current study's data showed that treating AD-modeled nematodes with CBD improved neuronal integrity and lifespan.

3.3.2 Trazadone

The second DOI investigated was Trazodone (TRA), which is a compound that has been commercially available now for over 50 years. It was initially prescribed to patients with depression due to it being a serotonin antagonist and reuptake inhibitor (SARI; Agnoli, 1986). Trazodone is rapidly taken up and undergoes Phase I Biotransformation through the cytochrome P450 3A4 (CYP3A4) and cytochrome P450 2D6 (CYP2D6) isoenzyme (Krystal, 2010). Following the metabolism of these isoenzymes, TRA transforms into the more active metabolite m-chlorophenylpiperazine (m-CPP; Melzacka et al., 1979). There is evidence to suggest that the metabolism of TRA is similar in the AD nematode model, as the model organism possesses the CYP13A7 ortholog to CYP3A4 (Chakrapani et al., 2008).

Some research has suggested repurposing TRA and SARI compounds may delay the onset of AD. One study found a 3-year delay in the showing of symptoms of AD in adults taking SARIs with mild cognitive impairment (Bartels et al., 2018). This connection of repurposing TRA as a translational compound for AD model *C. elegans* was in part the basis for including the drug as the second DOI in this research.

As stated, one of the main mechanisms of interest is the UPR pathway; TRA explicitly addresses the phosphorylation of the eIF2α-p pathway. There is evidence that TRA acts on the PERK pathway and ameliorates AD clinical symptoms. Some research has demonstrated that TRA is not only neuroprotective but has also improved behavioral deficits in p-Tau aggregation mouse models by acting on the PERK pathway on eIF2α-p during periods of chronic stress (Halliday et al., 2017; Moreno et al., 2013; Radford et al., 2015). These findings regarding TRA's ability to inhibit the phosphorylation of the eIF2α-p pathway made it the obvious choice for the second drug of interest to be employed in this study.

3.4 Nematodes

3.4.1 Maintenance

As noted in Section 3.1.2, the AD-model nematodes utilized for this research were obtained from the CGC at the University of Minnesota. The nematodes were grown on Nematode Growth Media (NGM) agar plates and stored in a 20 ℃ incubator. Nematodes were fed 200 µL of OP50, a nonpathogenic *Escherichia coli* (*E. coli*) strain, once a week. The maintenance for all of the various strains was equal. To keep the strains alive to propagate more, the "chunking" method was used. This involves sterilizing a metal spatula that is used to cut a small square in the NGM agar plate, which is then placed onto a new NGM plate. The newly propagated plates were also then fed with 200 µL of OP50.

3.4.2 Synchronization

In order to study age-specific nematodes, the nematodes were first washed from the NGM plates using M9 buffer and glass serological pipettes after which they were collected in either a 50 mL or 15 mL conical. The nematodes were then synchronized using 1 M NaOH and 5.25% hypochlorite bleaching treatments in 1.5 mL microcentrifuge tubes and spun for 1 min at 2000 rpm. This process kills everything excluding the eggs. Nematode pellets were then transferred from the 1.5 mL microcentrifuge tubes onto Petri dishes containing agar using 5-in glass aspirator pipettes. Nematodes were then fed with 200 µL of OP50 for 24 hr to ensure all eggs had hatched and the animals aged at the same rate. To ensure all animals did not progenerate, they were exposed to 50 µL of sterilizing agent FUdR on Day 3 (see Fig. 3.1).

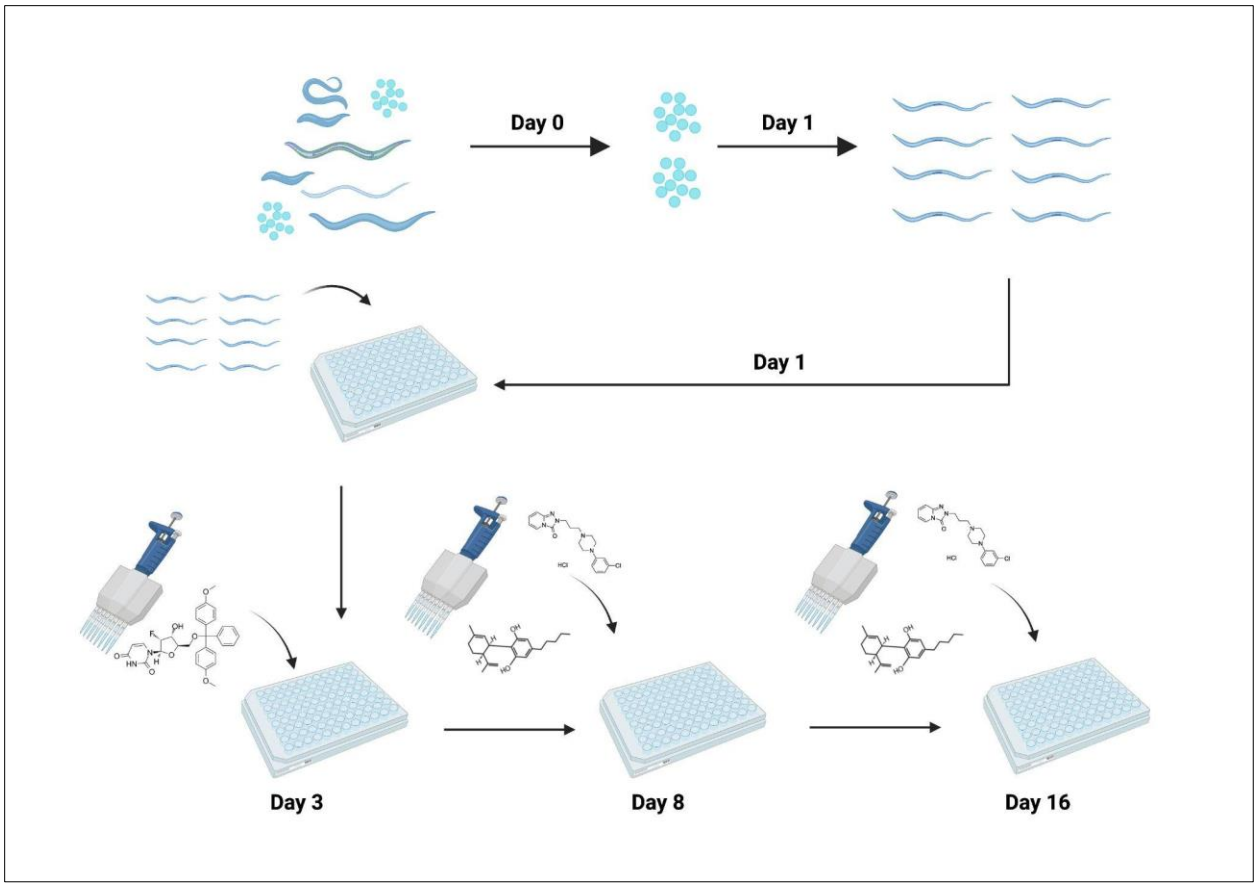

Figure 3.1. *Schematic Diagram Depicting Longevity Assay Method*

Note. Non-synchronous nematodes synchronized using a bleach solution that kills everything excluding the eggs. The eggs are then plated in a 96-well plate and treated with both compounds of interest and a sterilizing agent. Figure developed using information from Solis and Petrascheck (2011). Image created by author using BioRender.

3.5 Longevity Studies

The protocol used for this assay was adopted from Petrascheck lab (Solis & Petrascheck, 2011). The protocol was altered by the addition of drugs at separate time points in the lifespan of the nematodes to correspond with the different stages of life of the AD patient. Before drug stacking, *C. elegans* were plated in 96-well plates in S-complete buffer and treated to various concentrations of both drugs of interest. Three cohorts of nematodes were placed in three

separate wells, fed 10µL of 100 mg/mL of OP50 once a week, and counted every 3–5 days. Of these three cohorts, one was exposed for full-life, one was exposed on Day 8, and the last group was exposed on Day 16. From this pilot study, it was deduced that 100 µM TRA and 10 µM CBD seemed to be the most promising for extending the lifespan of the neurodegenerative strains. This process was then repeated using the drugs in combination. Due to both drugs acting upon the eIF2α-p pathway (Halliday et al., 2017; Melas et al., 2018), it was hypothesized that some additive effects would be seen.

Before studying combinational dosing, the nematodes were exposed to varying concentrations of either TRA or CBD at different time points to analyze both the optimal dose and time of exposure. Again, as previously discussed, the engineers of the $A\beta_{1-42}$ note that Day 8 is the middle age of the Pro-Aβ Aggr. model and the presence of $A\beta_{1-42}$ peaks at Day 12 (Fong et al., 2016). The time points used for this study were Day 1, Day 8, and Day 16. For our control group of nematodes, we exposed the animals to the highest volume of dimethyl sulfoxide (DMSO) they would have received if they were in the CBD-treatment groupings. It should also be noted that all of the DMSO values calculated per well were 0.6%, this is because wells containing more than 0.6% would be toxic to the nematodes. We included full-life exposure to ensure that our compounds were not toxic to our animals. The pilot study found the most beneficial doses for the two drugs were 100 µM TRA and 10 µM CBD. For the neurodegenerative strain, this research deduced that Pro-Aβ Aggr. had benefit from Day 8 treatment (see Figs. 5.1–5.2, Panel D) with 100 µM of TRA or 10 µM CBD, which significantly improved the lifespan of the nematodes incrementally at all future exposure time points across the lifetime (see Figs. 5.1–5.2, Panel F). For our Pro-Tau Aggr., 100 µM TRA significantly improved the lifespan at both Day 8 and Day 16 treatment (see Fig. 5.1, Panels J and L) and 10

µM CBD for full-life exposure (see Fig. 5.2, Panel G). These findings guided our research to potential therapeutic ranges when implementing combinational treatment for the subsequent neuronal integrity assays.

3.6 Touch Test Studies

In order to screen the nematodes for optimal dosages of the compounds of interest, *C. elegans* were allowed to grow on plates containing the isolated drug compounds at varying dosages for 1 week. The doses investigated for CBD included 1 µM, 5 µM, 10 µM, and 100 µM. The doses investigated for TRA were 25 µM, 50 µM, 100 µM, and 200 µM. Non-synchronous adults were then screened by employing a touch test assay. We targeted the anterior ventral process B interneuron (AVB), posterior ventral process C interneuron (PVC), anterior ventral process A interneuron (AVA), and anterior ventral process D interneuron (AVD). The AVB and PVC interneurons had the downstream effect of backward movement, while the AVA and AVD had the downstream effect of forward movement.

To conduct this stage of the study, agar plates containing varying concentrations of isolated compounds of either TRA or CBD were created. Nematodes were then exposed to each drug for 1 week and then subjected to a touch test. The motility of our experimental models of nematodes improved with 100 µM and 200 µM doses of TRA (see Fig. 4.1, Panels A–B). Our experimental strain's motility was also significantly improved with 5 µM and 10 µM CBD exposure (see Fig. 4.1, Panel C). We then investigated combinational doses of less than 100 µM TRA and greater than 5 µM CBD from this pilot work. The reason for reducing TRA concentration and increasing CBD concentration was due to the therapeutic indexes of each drug. Ideally, we would see either an additive or synergistic effect on the nematode’s motility with the combinational treatment.

Following this pilot screening, the data suggested that 100 µM and 200 µM TRA had the most significant effect in elucidating healthy motility (see Fig. 4.1, Panels A–B). For CBD, the data suggested that dosages of 5 µM and 10 µM had the most significant effect in elucidating healthy motility (see Fig. 4.1, Panel C). Based on both these and the longevity studies, we proceeded to conduct the touch test assay on *C. elegans* exposed to the combination of TRA and CBD. For the full-life assay, nematodes were exposed to the combination of drugs at Day 1 and then subjected to touch test on Day 7. To analyze motility response, the nematodes were synchronized to ensure they were the same age; the middle-age nematodes were exposed on Day 8 and experimented upon on Day 12. The last treatment group for late stage rescue were treated on Day 16 and tested on Day 18. These days were specifically chosen because, based on the previous literature, our Pro-Aβ Aggr. would be considered middle-aged at Day 8, the point where concentrations were observed to be at half maximum. According to the literature, Day 12 is when concentrations peak and when neurodegenerative strains seem to exhibit the most clear signs of neurodegeneration (Fong et al., 2016).

3.7 LC-MS/MS Drug Identification

In order to assure that our drugs of interest were making their way into the nematode, LC-MS/MS analytical chemistry was utilized. *C. elegans* were placed on plates containing either vehicle or combinational compounds to analyze this. The nematodes were then analyzed on Day 1, Day 8, or Day 16. Both pellets consisting of nematodes and washes used were saved. Pellets were washed to ensure that the LC-MS/MS nematodes analyzed compounds were washed to ensure compounds being analyzed derived solely from the pellet. Nematodes were washed from Petri-dishes using M9 buffer and 10 mL glass serological pipette. They were then transferred to 15 mL conical, which was filled with M9 buffer (15 mL) and centrifuged at 2000 rpm for 10

min. The pellet then underwent acetonitrile extraction and was transferred into a vial. Internal standards were added into our extractions as a control to ensure that retention times matched the drugs we were analyzing. Washes were extracted using borate buffer and butyl chloride. Wash extractions also had internal standard added to ensure protocol was done properly.

To ensure the compounds of interest were making their way into the nematode itself for our research, the nematodes were washed thoroughly through centrifugation and the implementation of liquid-liquid extraction. Through this process, we concluded that the drugs were, in fact, in the pellet of the nematodes through qualitative analysis using LC-MS/MS. In the first attempt to analyze the pellet for TRA and CBD, we could not confirm that the drugs made their way into the pellet since both compounds were also in the wash. Because of this, it was hypothesized that increasing the number of washes with PBS to 25 centrifuges would clear any drug in the wash.

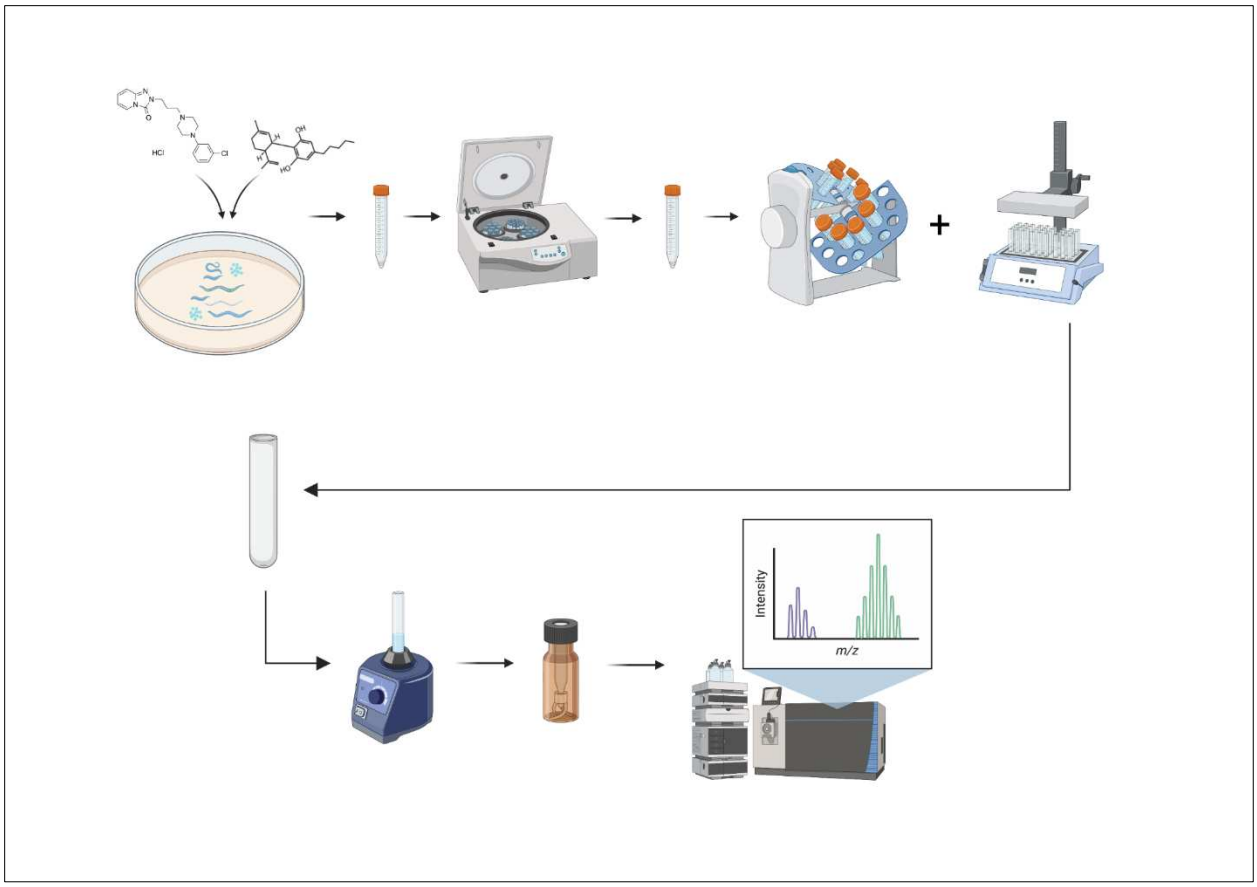

Figure 3.2. *Schematic Diagram Depicting LC-MS/MS Drug Identification*

Note. Nematodes are placed on plates containing the drugs of interest and then washed multiple times. Image created by author using BioRender.

3.8 Antibody Staining

To achieve antibody staining in the nematodes, we adopted the freeze-cracking protocol (Duerr, 2013). This is because the cuticle surrounding the nematode is impervious to staining. This cracking is achieved by first washing the nematodes from the NGM plates using a glass pipette into a 15 mL conical. The conical is then centrifuged at 3000 rpm for 10 min. The nematodes are vortexed on high for roughly 10 s in between centrifuges. This process is done a total of three times in order to rinse the nematodes free of bacteria. After the centrifuge process is

completed, a 9-in. aspirator pipette is used to transfer the pellet of nematodes into a 1.5 mL Eppendorf tube. The tube is then adjusted with twice the sterile water compared to the pellet. Once this has been done, 25 µL of the solution is added to charged slides. The slides then have a coverslip placed on them and are placed on a metal sheet sitting directly on top of dry ice. After 5 min, the slides are taken off the metal sheet and separated from each other with one swift motion. The charged slide is then placed on a slide holder and subjected to light fixation. The light fixative includes 2 min of sitting in 100% methanol, followed by 4 min of 100% acetone, and finally placed in 1x PBS. After the light fixative process is complete, the nematodes are then stained with the antibodies of interest.

The actual staining process of *C. elegans* included two antibodies that stained for either A$\beta_{1\text{-}42}$ or p-Tau. The third stain used was 4′,6-diamidino-2-phenylindole (DAPI), which was utilized both as a morphological marker and as an internal standard to make sure our methods properly worked. The stain used for A$\beta_{1\text{-}42}$ was beta-Amyloid (1-42) polyclonal antibody (Thermo Fisher Scientific), which marked the amino acids 36–42 C-terminal region. The antibody used for Tau was AT270 (Thermo Fisher Scientific), a p-Tau marker that analyzed the Thr181 nucleotide region. The beta-Amyloid (1-42) polyclonal antibody marker was used at a 1:400 ratio whereas AT270 was used at a 1:2000 ratio. Both of the antibody mixes for the A$\beta_{1\text{-}42}$ and p-Tau markers were placed with 600 µL on the corresponding models and placed in refrigeration at 4 °C overnight. For DAPI, we used a 1:2000 ratio and it was placed with 600 µL at room temperature on all nematodes for no more than 3 min.

CHAPTER 4

NEURONAL INTEGRITY ASSAY

4.1 Introduction to the Motility Assay

For this experiment, we analyzed the function of the AVA, AVD, AVB, and PVC interneurons. The AVA and AVD interneurons, when exposed to stimuli, are expressed as backward motion. The AVB and PVC neurons, when exposed to stimuli, are expressed as forward movement (Eisenmann, 2005). If the nematode did not react to forward or backward stimuli, it was recorded as "not responding." These transgenic models did not respond correctly to the stimuli due to the aggregation of proteins as the nematodes aged (Fatouros et al., 2012).

It should be noted that the engineers of our Pro-Aggr. Aβ strain did not specifically look at stimuli response but rather observed sinusoidal movement and noted no difference in motility before Day 8 (Fong et al., 2016). Given the evidence that both motility and neuronal aggregates correlated to overall less response, we employed a gentle touch test assay on the AVA, AVD, AVB, and PVC interneurons to determine the necessary doses that improve motility for the neurodegenerative nematode model.

4.2 Experimental Setup: Isolated Treatment Touch Test

Non-synchronous adult nematodes were exposed to NGM-treated agar plates treated with isolated drug (TRA or CBD) for 1 week at varying doses and then subjected to the gentle touch test assay. The overall goal for this assay was to deduce appropriate doses for each drug and affirm that our neurodegenerative nematodes were appropriate for use in this assay. The first

aspect of the research that must be noted is that the neurodegenerative nematodes had significantly worse motility. Fleeing from both stimuli was recorded as a 100% response.

The gentle touch test found that the neurodegenerative strains of *C. elegans* have significantly worse motility. Nematodes were plated on NGM agar Petri dishes treated with either vehicle or varying concentrations of TRA and fed 200 µL OP50 (see Fig. 4.1, Panels A–B). After 1-week exposure, nematodes were subjected to a gentle touch test, specifically to repeatedly target the AVB and PVC interneurons. Failure to flee from either stimulus was recorded as 0%. Statistical analyses were performed using a two-way ANOVA to compare the Pro Aggr. strains with their control counterparts. This information is presented on Panel A of Figure 4.1.

Next, nematodes were plated on NGM agar Petri dishes treated with either the vehicle or varying concentrations of CBD and fed 200 µL OP50 (see Fig. 4.1, Panels C–D). After 1-week exposure, the nematodes were subjected to a gentle touch test, specifically to repeatedly target the AVB and PVC interneurons. Failure to flee from either stimulus was recorded as 0%. Statistical analyses were performed using a two-way ANOVA, comparing the Pro Aggr. strains with their control counterparts.

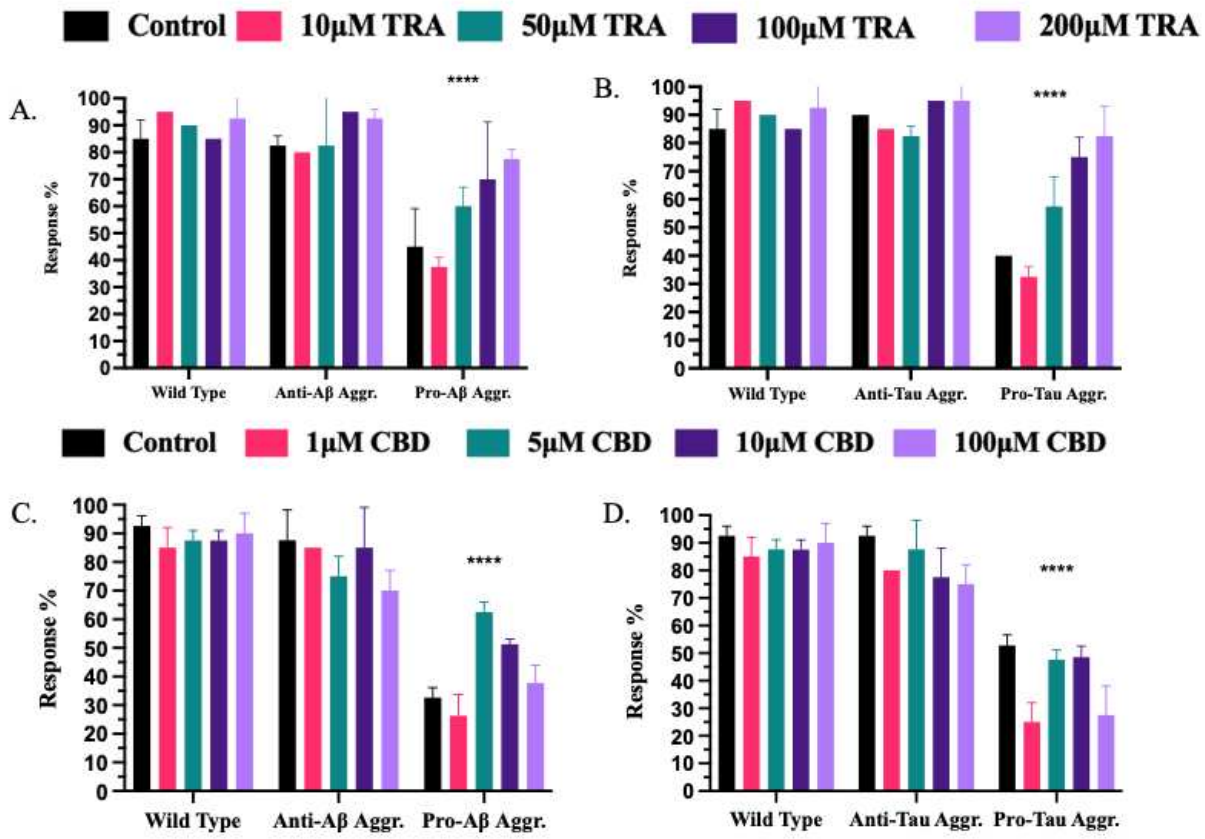

Figure 4.1. *Gentle Touch Test on Non-Synchronous Adult* C. elegans *Exposed to Isolated Compounds*

Note. Wild Type (n = 120), Anti-Aβ Aggr. (n = 120), and Pro-Aβ Aggr. (n = 120). Results are presented in a two-way ANOVA CI interval.
****$p < 0.0001$.

4.3 Experimental Setup: Combinational Treatment Touch Test

Age synchronous adult nematodes were exposed to NGM-treated agar containing 10 µM CBD and 100 µM TRA The overall goal for this assay was to assess how treatment with both drugs of interest phenotypically manifested days after exposure. We investigated full-life exposure in which nematodes were treated with the combination on Day 1 of their lives and tested 1 week later. After identifying the most significant doses of TRA and CBD (see Fig. 4.1),

we then exposed all strains to full-life exposure starting Day 1 and then a touch test assay on Day 7. For Day 12 touch test, nematodes were treated on Day 8. Finally, Day 18 touch test was analyzed after a 2-day treatment that began on Day 16. Day 12 was a point of interest due to the peak of Aβ1-42 aggregation (Fong et al., 2016). We investigated this to see the potentiation of late-stage rescue. For this experiment, we used the previous criteria of fleeing from both stimuli as a 100% response. In addition, a harsh touch test utilizing a titanium pick for the harsh touch test was added to investigate the sensitivity of neurons post-gentle touch test (McClanahan et al., 2017).

Our findings were that at Day 7, all strains had no change in response (see Figs. 4.2–4.5). For both our control strains, Anti-Aβ Aggr. and Anti-Tau Aggr., none of the treatments significantly changed the percent response between combinational treatment and vehicle (see Figs. 4.2–4.5). The following series of figures present the Day 7 combinational treatment touch test results.

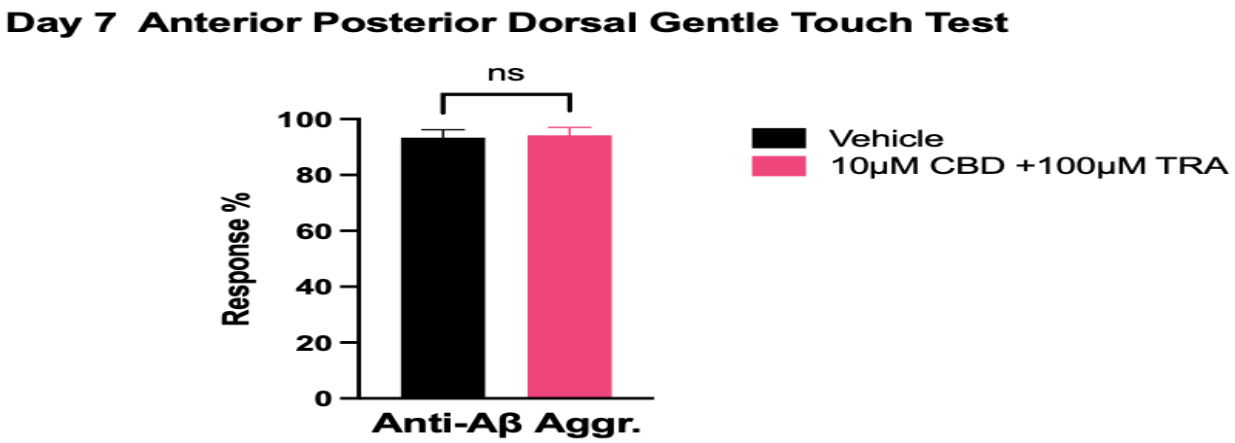

Figure 4.2. *Gentle Touch Test Response of Anti-Aβ Aggr. After 4-Day Exposure to Combinational Drug-Treated NGM Agar Plates*

Note. Results are presented as a paired two-tailed *t*-test adjusted to *p*-value.

As shown in Figure 4.2, there was no significant difference in the motility response of Anti-Aβ Aggr. to the gentle touch test after 7 days of exposure to the combinational treatment as compared to the vehicle treatment. Furthermore, there was no significant response to the gentle touch test by the Anti-Aβ Aggr. strain on Day 7 of either vehicle or combinational treatment.

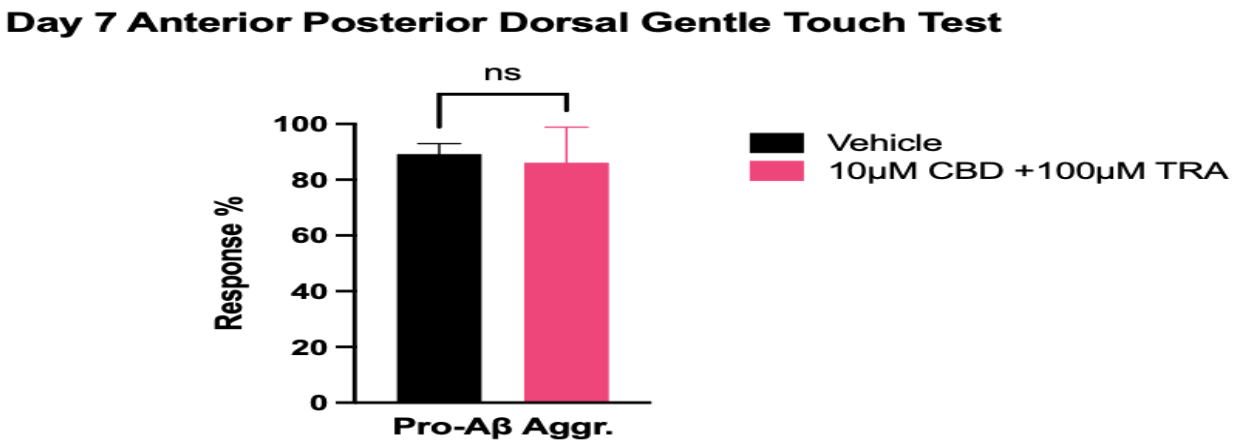

Figure 4.3. *Gentle Touch Test Response of Pro-Aβ Aggr. After 7-Day Exposure to Combinational Drug-Treated NGM Agar Plates*

Note. Results are presented as a paired two-tailed *t*-test adjusted to *p*-value of < 0.05.

Figure 4.3 presents the findings regarding the gentle touch test on the Pro-Aβ Aggr. strain after 7 days of exposure to the combinational treatment. Specifically, we found no significant motility response in the Anti-Aβ Aggr strain as compared to the response with either vehicle or combinational treatment. As compared to the vehicle treatment, there was no significant difference in the motility response to the gentle touch test of Anti-Tau Aggr. after 7-day exposure to the combinational drug treatment (see Fig. 4.4).

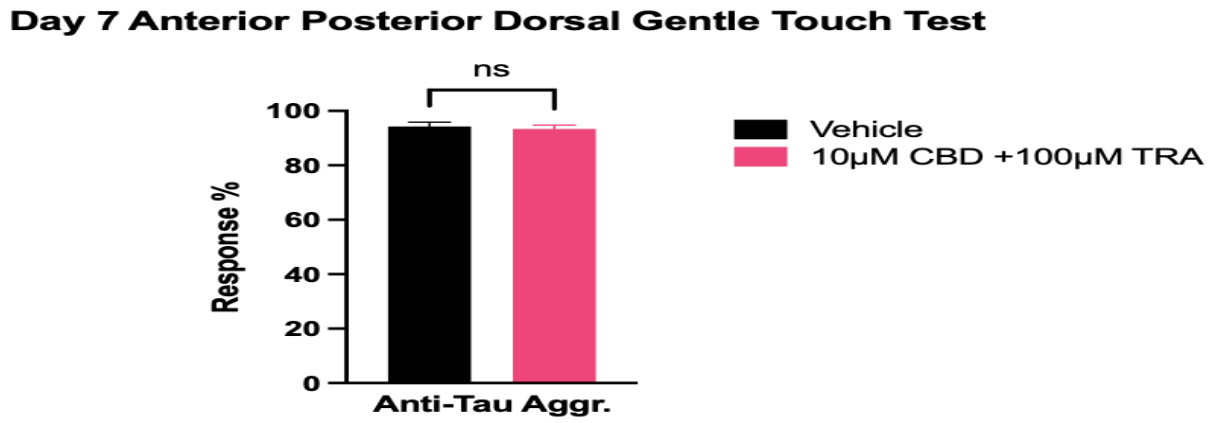

Figure 4.4. *Gentle Touch Test Response in Anti-Tau Aggr. After 7-Day Exposure to Combinational Drug-Treated NGM Agar Plates*

Note. Results are presented as a paired two-tailed *t*-test adjusted to *p*-value.

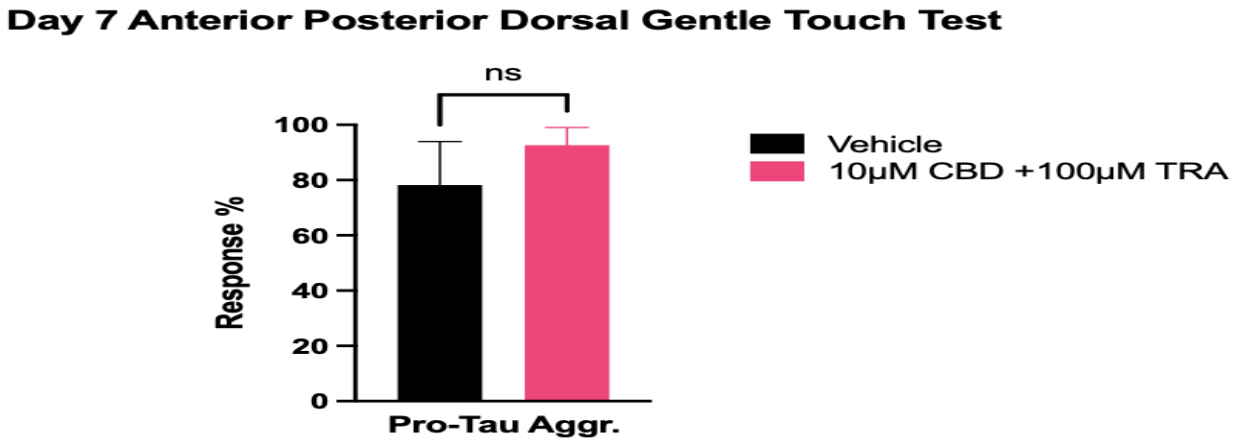

Figure 4.5. *Gentle Touch Test Response of Pro-Tau Aggr. After 7-Day Exposure to Combinational Drug-Treated NGM Agar Plates*

Note. Results are presented as a paired two-tailed *t*-test adjusted to *p*-value.

Figure 4.5 presents the findings regarding Pro-Tau Aggr. strain's response to the gentle touch test after 7 days of exposure to the combinational drug treatment, which found no significant motility response as compared to either the vehicle or combinational treatment.

For the Pro-Aβ Aggr. strain exposed to the combination of TRA and CBD on Day 8, response to both gentle and harsh tests significantly improved after 4 days of exposure when the tests were conducted on Day 12 (see Fig. 4.6, Panels A and E). At Day 18, our Pro-Aβ Aggr. had significantly improved response after 2 days of exposure to the combination of TRA and CBD (see Fig. 4.6, Panels C and G). The Pro-Tau Aggr. had significantly improved response for harsh touch test at Day 18 after a 2-day exposure (see Fig. 4.6, Panel H), but did not significantly improve response to the gentle touch test after a 2-day exposure (see Fig. 4.6, Panel D).

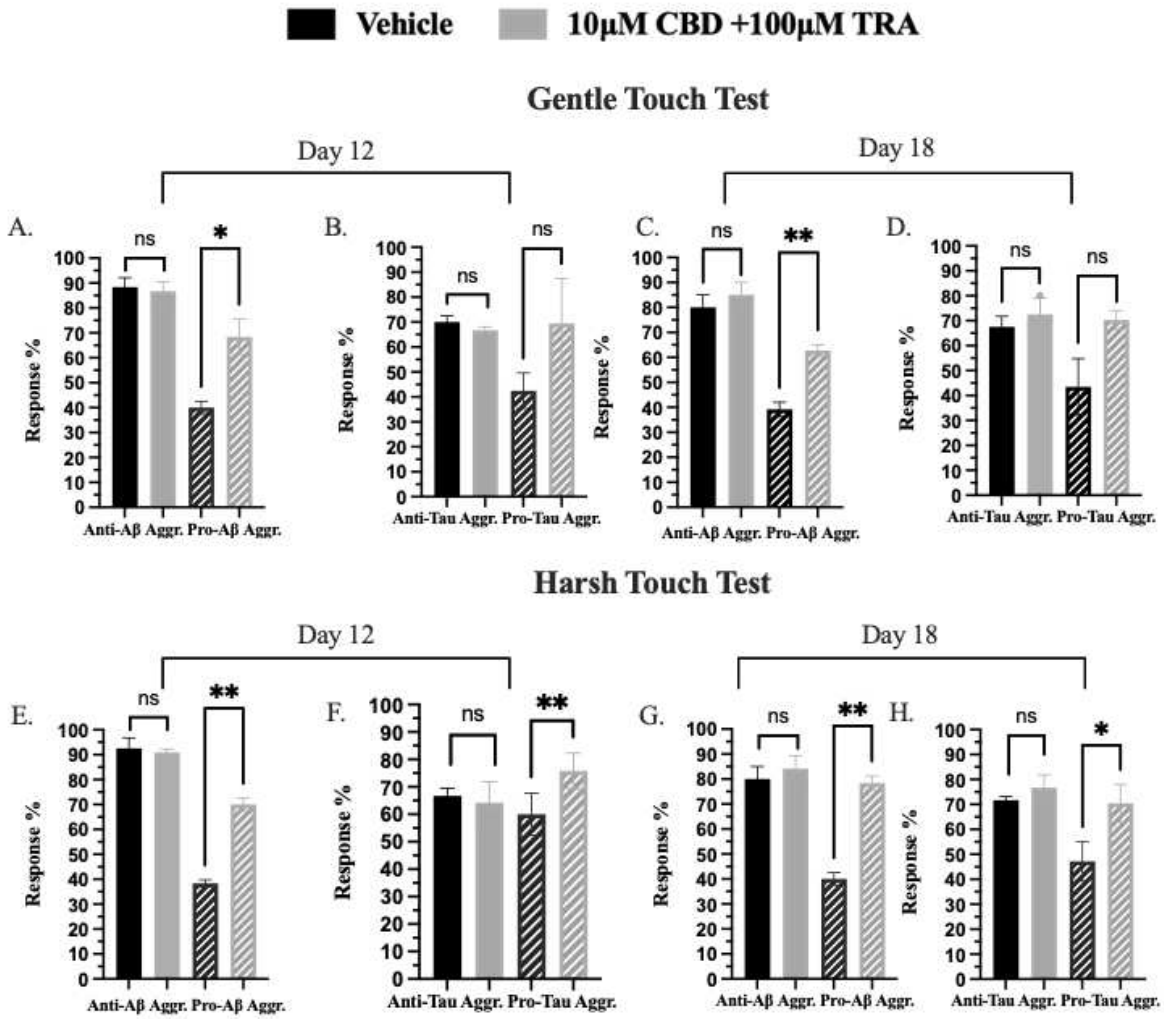

Figure 4.6. *Gentle Touch Test and Harsh Touch Test Responses of Synchronous Tau and* Aβ *to Combinational Drug-Treated NGM Agar Plates*

Note. Touches were repeated and scored as 100% response if *C. elegans* expressed both forward and backward fleeing. Statistical analyses were performed using paired *t*-test. Pro-Aβ Aggr. strains (n = 120), Anti-Aβ Aggr. (n = 120), Pro-Tau Aggr. strains (n = 120), and Anti-Tau Aggr. (n = 120).
*p < 0.05.
**p < 0.01.

Figure 4.6 presents the findings of the gentle and harsh touch tests conducted on the nematodes exposed to combinational treatments of 10 μM CBD and 100 μM TRA. Panel A presents the results of the gentle touch test on Aβ model *C. elegans* exposed to the combinational treatment on Day 8 and then tested on Day 12. The results of this gentle touch test on Tau model *C. elegans* on AVB and PVC interneurons exposed to the combinational treatment on Day 8 and tested on Day 12 are shown on Panel B. The gentle touch test results for Aβ model *C. elegans* on AVB and PVC interneurons exposed to the combination of TRA and CBD on Day 16 and tested on Day 18 are shown on Panel C. Please see Panel D for the results of the gentle touch test on Tau model *C. elegans* on AVB and PVC interneurons exposed to the combinational TRA and CBD treatment on Day 16 and tested on Day 18.

The harsh touch test results were as follows. For Aβ model *C. elegans* on AVB and PVC interneurons exposed to the combination of TRA and CBD on Day 8 and tested on Day 12, see Panel E. For Tau model *C. elegans* on AVB and PVC interneurons exposed to the combination of TRA and CBD on Day 8 and tested on Day 12, see Panel F. For Aβ model *C. elegans* on AVB and PVC interneurons exposed to the combinational treatment on Day 16 and tested on Day 18, see Panel G. And finally, for Tau model *C. elegans* on AVB and PVC interneurons exposed to the combination of TRA and CBD on Day 16 and tested on Day 18, see Panel H.

CHAPTER 5

LONGEVITY ASSAY

5.1 Chapter Introduction

Alzheimer's disease is a condition that decreases the overall lifespan of the individual (Zanetti et al., 2009). We tested the life expectancy of our AD-modeled nematodes utilizing 96-well adopted from the Petrascheck lab (Solis & Petrascheck, 2011). We first analyzed the lifespan of the nematodes using isolated doses of TRA and CBD. The nematode day of treatment included full-life treatment, Day 8 treatment, and Day 16 treatment. The decision to dose the nematodes for full-life, Day 8, and Day 16 was based on the dates of behavioral deficits and aggregation peak (Fong et al., 2016), meaning Day 8 treatment would reveal the interactions of our drugs prior to Aβ aggregation, and Day 16 would reveal potentiation for late-stage rescue.

5.2 Longevity Assay Results

The results of the longevity assay are fully presented on Figures 5.1 and 5.2. As stated in Section 3.5 of the methodology, the worms were placed into a 96-well and counted every 3–5 days to see if they were alive or not; worms were counted until all had died. Survival statistics were run using Mantel–Cox test and the results of the isolated TRA and CBD treatments were compared to those of the vehicle treatment.

The findings regarding TRA (see Fig. 5.1) were as follows. Panel A of the figure shows the full-life TRA treatment lifespan results for Anti-Aβ Aggr. *C. elegans*. Survival statistics were run using Mantel–Cox test, which found a significant effect of $p < 0.01$ for the 50 µM and 100 µM TRA treatments. On Panel B, full-life TRA treatment lifespan results on Pro-Aβ Aggr. *C. elegans* are presented. Mantel–Cox test found $p < 0.05$ for the 100 µM TRA treatment. Panel C

presents the lifespan results on Day 8 of TRA treatment for Anti-Aβ Aggr. *C. elegans*; no significant difference was observed between vehicle and treatment groups. The Day 8 TRA treatment lifespan results on Pro-Aβ Aggr. *C. elegans* are presented on Panel D. Mantel–Cox test found $p < 0.0001$ for the 100 µM TRA treatment. On Panel E, the results for Day 16 TRA treatment lifespan for Anti-Aβ Aggr. *C. elegans* are shown. The results on Day 8 for the TRA lifespan treatment on Pro-Aβ Aggr. *C. elegans* using Mantel–Cox test found $p < 0.0001$ for the 100 µM TRA (see Panel F). Panel G presents the data on full-life TRA treatment on Anti-Tau Aggr. *C. elegans*. The data on the full-life TRA treatment lifespan results on Pro-Tau Aggr. *C. elegans* are presented on Panel H; the Mantel–Cox test found $p < 0.01$ for both 25 µM TRA and 50 µM TRA. On Panel I, Day 8 TRA treatment lifespan results on Anti-Tau Aggr. *C. elegans* are presented; Mantel–Cox test found $p < 0.05$ for 100 µM TRA. The Day 8 TRA treatment lifespan results on Pro-Tau Aggr. *C. elegans* statistics are shown on Panel J; Mantel–Cox test found $p < 0.05$ for 25 µM TRA and $p < 0.001$ for 100 µM TRA. Next, on Panel K, Day 16 TRA treatment lifespan results on Anti-Tau Aggr. are shown. Finally, Panel L presents the Day 16 TRA treatment lifespan results on Pro-Tau Aggr. *C. elegans*; Mantel–Cox test found $p < 0.01$ for 50 µM TRA and $p < 0.0001$ for 100 µM TRA. The data suggest that the neurodegenerative strains lived longer with different doses at all times of exposure.

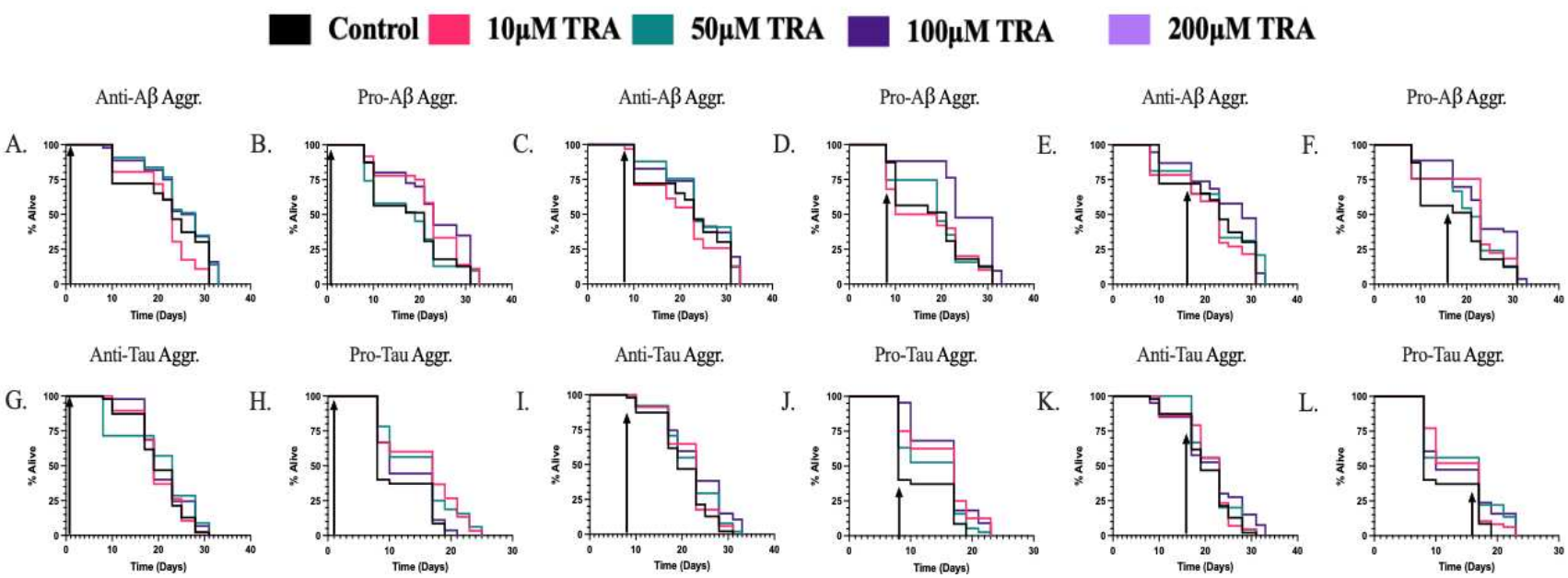

Figure 5.1. *Longevity Analysis of Varying Dosages of TRA on All Nematode Strains*

Note. Results are presented as a Mantel–Cox test. Black arrow indicates time at which doses were given. Nematodes were fed once a week on 10 mg/mL *E. coli* OP50. The ~n = 10 per well (in three separate wells). The controls registered no change and therefore no p-values are indicated for Panels C, E, G, K. Based on the dosage and as described in the associated narrative, some panels involve more than one p-value. P-values for each panel are:
$p < 0.05$: Panels B, I, and J.
$p < 0.01$: Panels A, H, and L.
$p < 0.001$: Panel J.
$p < 0.0001$: Panels D, F, and L.

This section will describe the data presented on Figure 5.2, which shows the lifespan results for CBD. As with the TRA longevity assay, worms (total of ~n = 30, 10 in each of three separate wells) were placed into a 96-well and were fed 10 mg/mL *E. coli* OP50. The nematodes were then counted every 3–5 days to see if they were alive or not. Worms were counted until all had died. Statistics were run using Mantel–Cox test to compare to the vehicle treatment.

1. Panel A shows full-life CBD treatment lifespan results on Anti-Aβ Aggr. *C. elegans*.
2. Panel B shows full-life CBD treatment lifespan results on Pro-Aβ Aggr. *C. elegans*. Mantel–Cox test found $p < 0.01$ for 10 µM CBD treatment.
3. Panel C shows Day 8 CBD treatment lifespan results on Anti-Aβ Aggr. *C. elegans*.
4. Panel D shows Day 8 CBD treatment lifespan results on Pro-Aβ Aggr. *C. elegans*. Mantel–Cox test found $p < 0.001$ for 1µM CBD, $p < 0.01$ for 5 µM CBD, and $p < 0.0001$ for 10 µM CBD.
5. Panel E shows Day 16 CBD treatment lifespan results on Anti-Aβ Aggr. *C. elegans*.
6. Panel F shows Day 16 CBD treatment lifespan results on Pro-Aβ Aggr. *C. elegans*. Mantel–Cox test found $p < 0.01$ for 5µM CBD and $p < 0.0001$ for 10µM CBD.
7. Panel G shows full-life CBD treatment lifespan results on Anti-Tau Aggr. *C. elegans*.
8. Panel H shows full-life CBD treatment lifespan results on Pro-Tau Aggr. *C. elegans*. Mantel–Cox found $p < 0.05$ for 1 µM CBD, $p < 0.05$ for 5 µM CBD, and $p < 0.0001$ 10 µM CBD.
9. Panel I shows Day 8 CBD treatment lifespan results on Anti-Tau Aggr. *C. elegans*.
10. Panel J shows Day 8 CBD treatment lifespan results on Pro-Tau Aggr. *C. elegans*. Mantel–Cox test found compared to vehicle treatment $p < 0.001$ for 1 µM CBD and $p < 0.05$ 5 µM CBD.

11. Panel K shows Day 16 CBD treatment lifespan results on Anti-Tau Aggr. *C. elegans*. Mantel–Cox test found compared to vehicle treatment $p < 0.05$ for 10 µM CBD.
12. Panel L shows Day 16 CBD treatment lifespan results on Pro-Tau Aggr. *C. elegans*. Mantel–Cox test found compared to vehicle treatment $p < 0.05$ for 5 µM CBD.

From this study, we found that not only was CBD not toxic, at certain doses it was beneficial for varying time points of exposure.

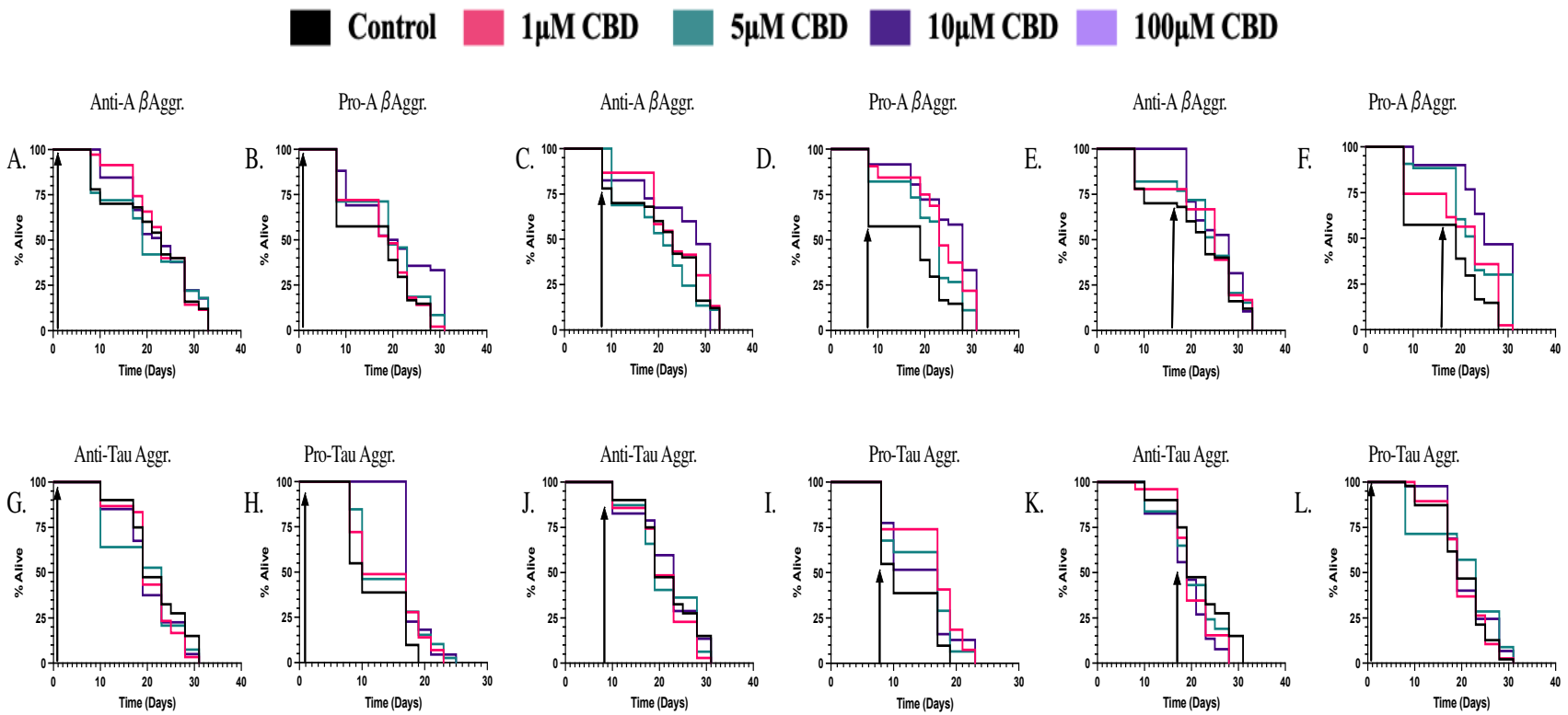

Figure 5.2. *Longevity Analysis of Varying Doses of CBD on all Nematode Strains*

Note. Results are presented as a Mantel–Cox test. Black arrow indicates time at which doses were given. Nematodes fed once a week on 10 mg/mL *E. coli* OP50. The ~n = 10 per well (in three separate wells). Some panels reflect more than one p-value and some panels reflect that no change was found.
$p < 0.05$: Panels H, J, K, and L.
$p < 0.01$: Panels B, D, and F.
$p < 0.001$: Panels D and J.
$p < 0.0001$: Panels D, F, and H.

CHAPTER 6

LC-MS/MS EXPERIMENTATION

6.1 Chapter Introduction

LC-MS/MS experimentation is widely used for many experiments and serves to verify both organic structure presence and investigate proteomics (Cabreiro et al., 2013). The purpose of utilizing LC-MS/MS for our research was to verify the presence of TRA and CBD in our nematodes. While vehicle treatments were used for all of our experiments, we believed that utilizing the LC-MS/MS machine would be a better method to validate the presence of drugs in the nematodes. We also believed that utilizing LC-MS/MS would open the door to further analyzing what metabolites were present in the nematodes. Unfortunately, identification of the drugs was more complicated than predicted. The issues encountered in the studies were primarily due to pellet size, washes, and the time it would take to analyze these models.

6.2 Conformation of TRA and CBD Using LC-MS/MS

In the first attempt at analyzing the presence of both CBD and TRA within the pellet, nematodes on NGM agar plates were treated with 10 µM CBD and 100 µM TRA. A pellet of nematodes was then collected after 1 day. The days the pellets were collected were correlated with the days of treatment for the longevity experiments. It was important to ensure that the drug made its way inside the nematode and that what was being analyzed was not in the pellet. Once the exposure time elapsed on the first attempt, nematodes were collected with autoclave water and centrifuged twice at 2000 rpm with fresh autoclaved water. The centrifuge's washes were incorporated into the analysis and it was determined both CBD and TRA were present in the wash, potentially contaminating our results. Figures 6.1–6.16 present the findings of the first

attempt of this experiment; we were unable to identify that the organic structures were inside the pellet due to the amount of substance still found in the washes. After extraction, the sample was run through a Kinetex 2.6 µm Phenyl-Hexyl LC column. We were unable to identify organic structures in the pellet because the washes had high levels of compounds (see Figs. 6.5–6.6); therefore, since both drugs were found in the pellet-exposed wash, it cannot be confirmed that what we found in the pellet were not essentially compounds located on the external of the *C. elegans*. Due to this finding, we hypothesized that utilizing PBS for washes and increasing the washes to 25 centrifuges would completely clear both TRA and CBD from the wash, allowing us to successfully assess the amount of the compounds internal to the *C. elegans* pellet.

(a)

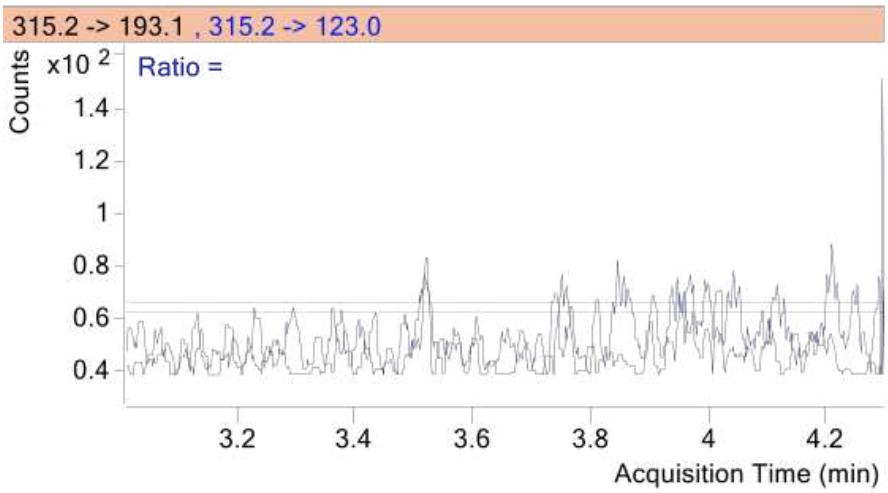

(b)

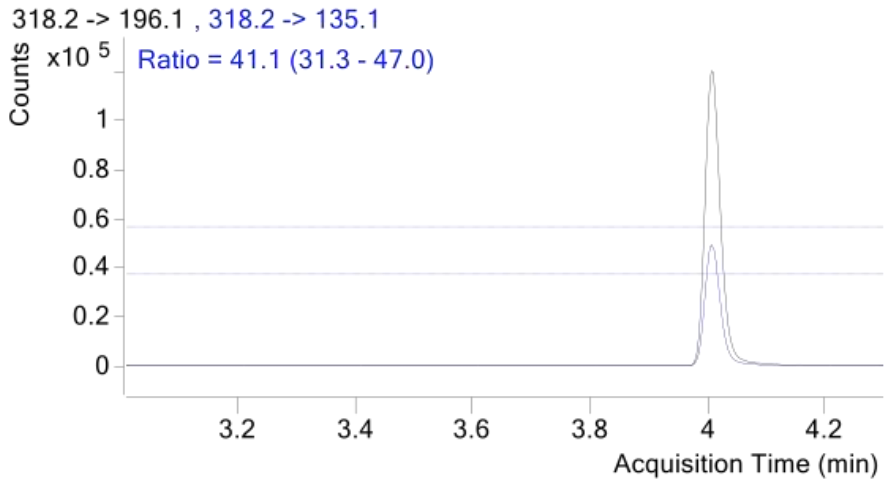

Figure 6.1. *Chromatogram of Pellet Exposed to DMSO for 1 Day: Conformation of CBD Presence*

Note. Figure 6.1(a) is the analysis of CBD whereas Figure 6.1(b) is the internal standard. One-day of exposure to the pellet shows no CBD found in the pellet.

(a)

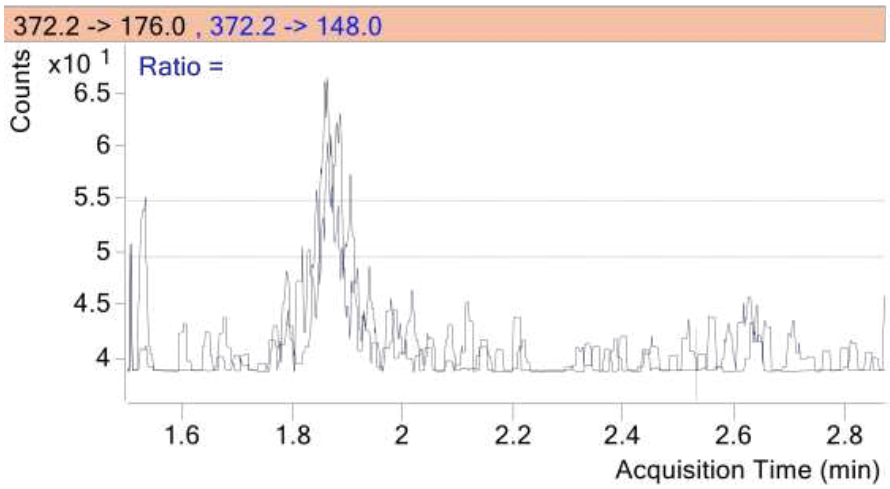

(b)

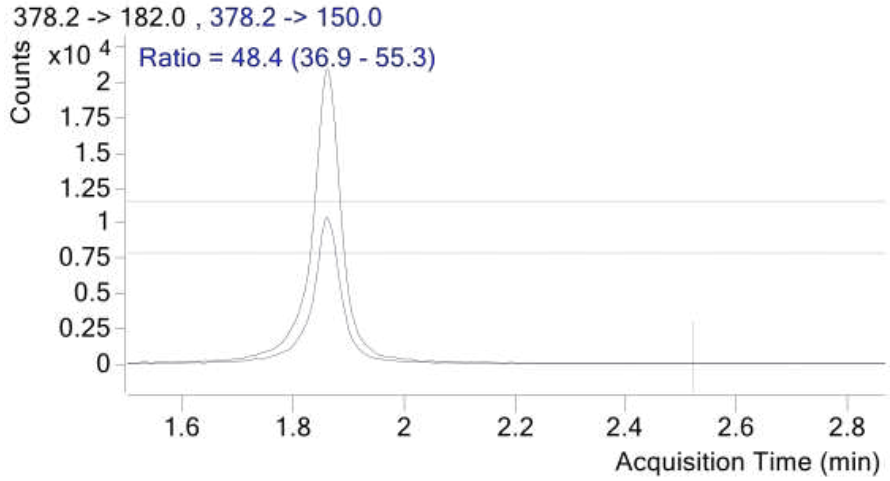

Figure 6.2. *Chromatogram of Pellet Exposed to DMSO for 1 Day: Conformation of TRA Presence*

Note. Figure 6.2(a) is the analysis of TRA whereas Figure 6.2(b) is the internal standard. One day of exposure shows no TRA found in the pellet.

(a)

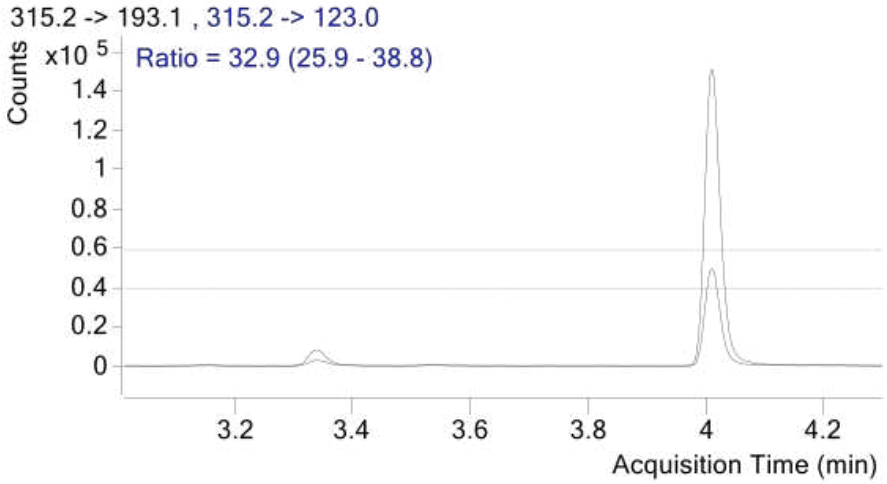

(b)

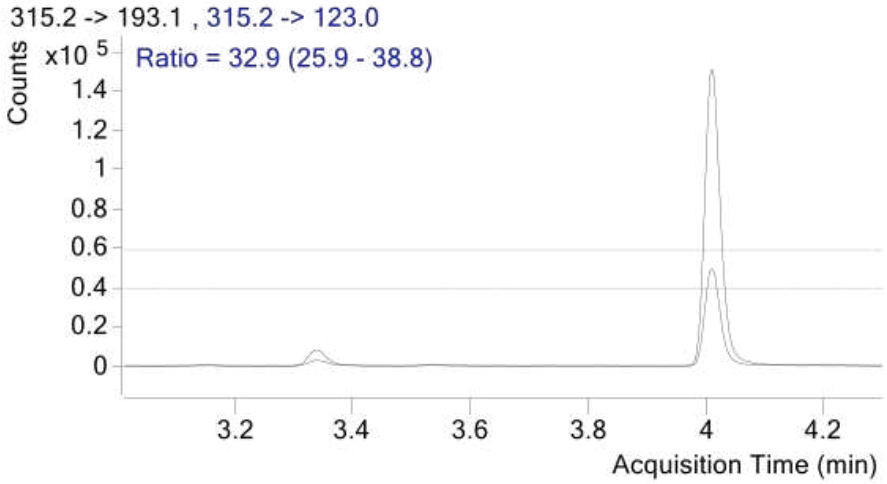

Figure 6.3. *Chromatogram of Pellet Exposed to 100 µM TRA and 10 µM CBD for 1 Day: Conformation of CBD Presence*

Note. Figure 6.3(a) is the analysis of CBD whereas Figure 6.3(b) is the internal standard. One day of exposure to the pellet shows both CBD and internal standard in the pellet extraction.

(a)

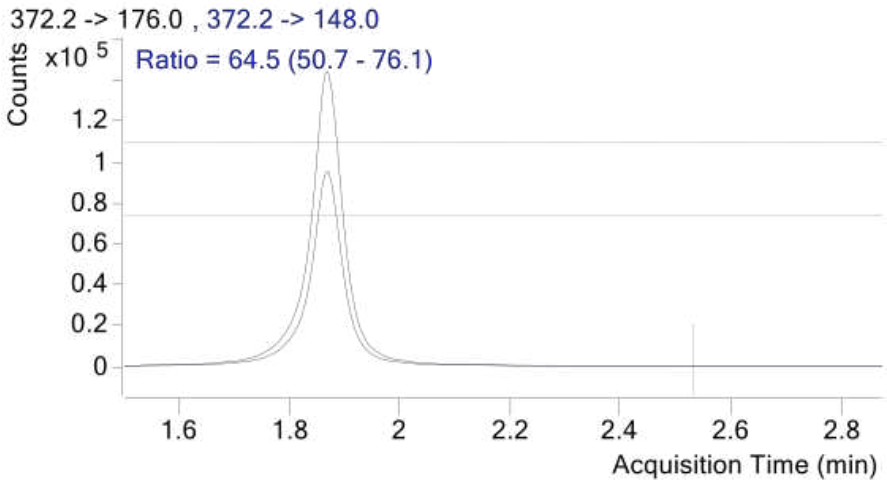

(b)

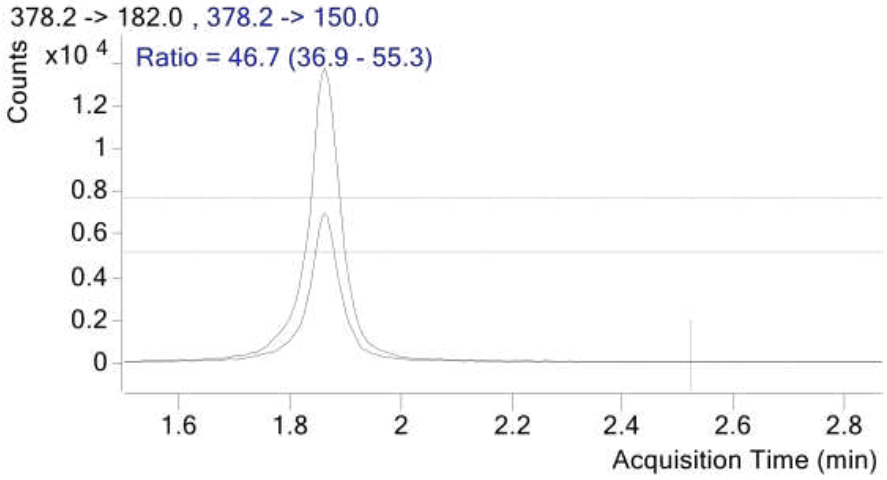

Figure 6.4. *Chromatogram of Pellet Exposed to 100 µM TRA and 10 µM CBD for 1 Day: Conformation of TRA Presence*

Note. Figure 6.4(a) is the analysis of TRA whereas Figure 6.4(b) is the analysis of the internal standard. One day of exposure to the pellet shows both TRA and internal standard in the pellet extraction.

(a)

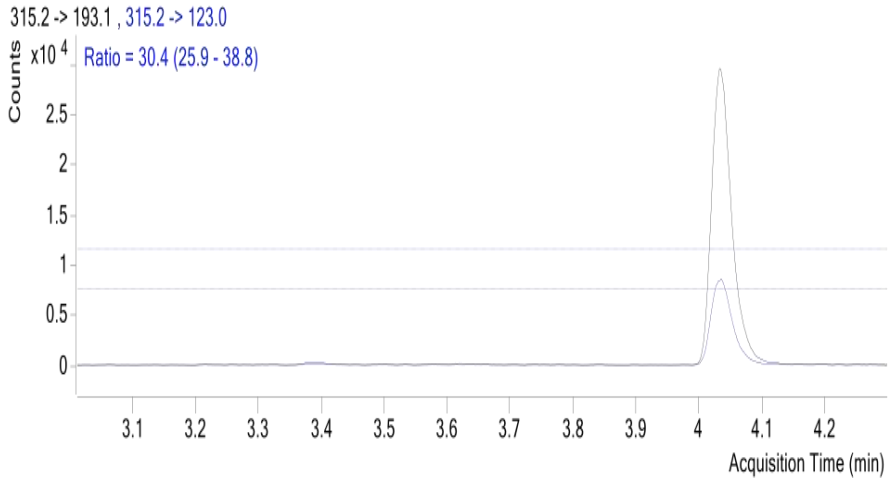

(b)

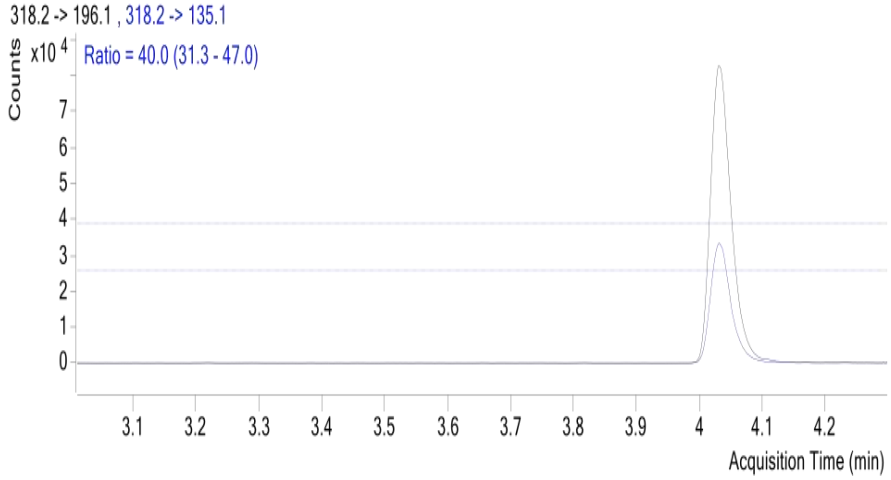

Figure 6.5. *Chromatogram of First Wash Exposed to 100 µM TRA and 10 µM CBD for 1 Day: Conformation of CBD Presence*

Note. Figure 6.5(a) is the analysis of CBD whereas Figure 6.5(b) is the internal standard. One day of exposure to the wash shows both CBD and internal standard in the pellet extraction.

(a)

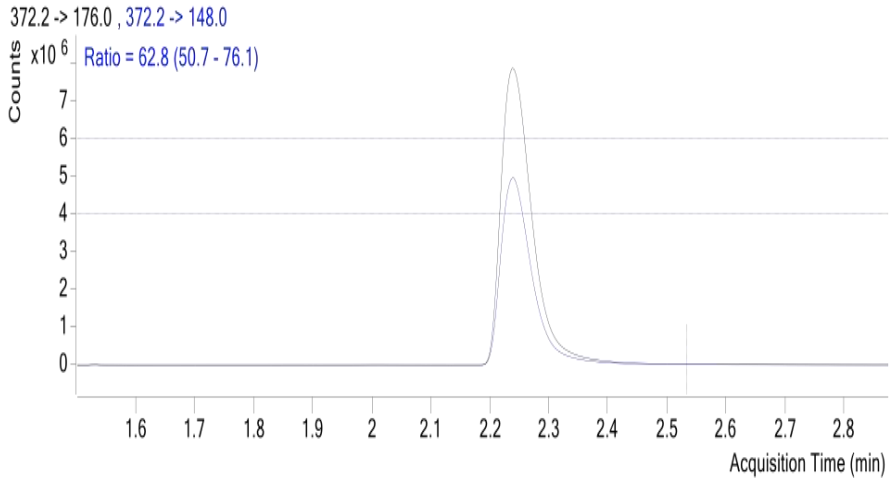

(b)

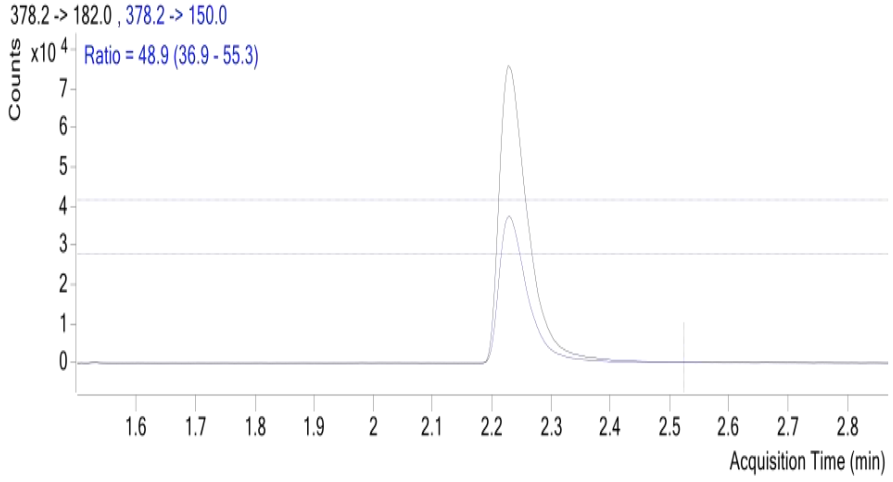

Figure 6.6. *Chromatogram of First Wash From Pellet Exposed to 100 µM TRA and 10 µM CBD for 1 day: Conformation of TRA Presence*

Note. Figure 6.6(a) is the analysis of TRA whereas Figure 6.6(b) is that of the internal standard. One day of exposure to the wash shows both TRA and internal standard in the wash extraction.

(a)

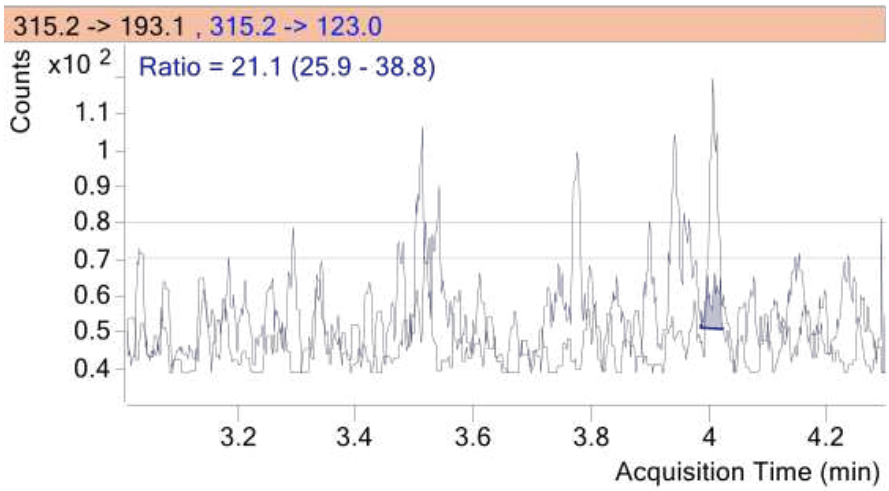

(b)

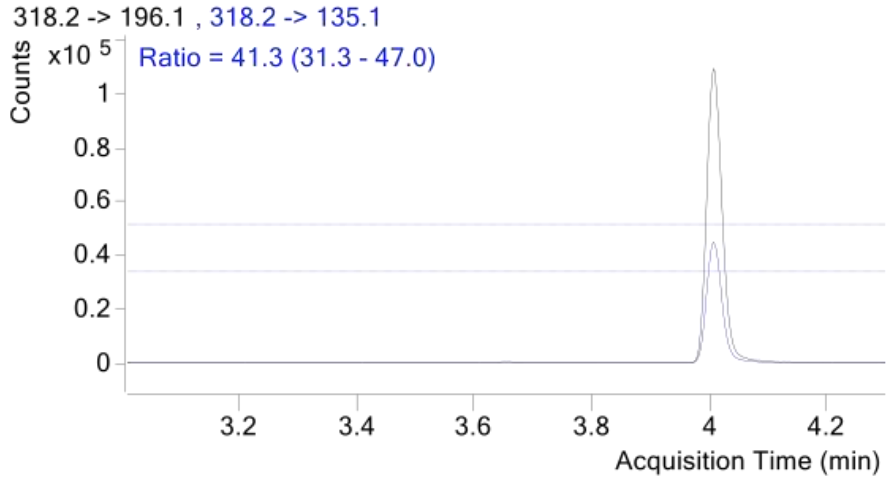

Figure 6.7. *Chromatogram of Pellet Exposed to DMSO for 8 Days: Conformation of CBD Presence*

Note. Figure 6.7(a) is the analysis of the CBD whereas Figure 6.7(b) is that of the internal standard. Eight days of exposure to the pellet shows no CBD.

(a)

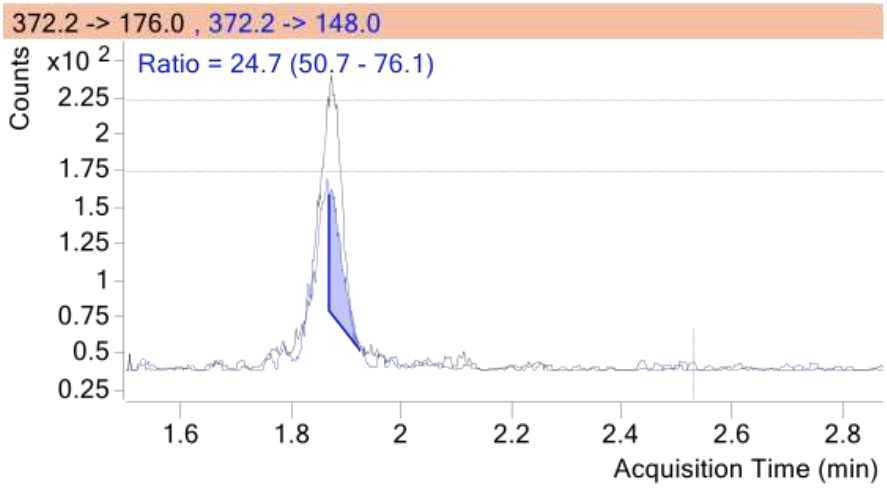

(b)

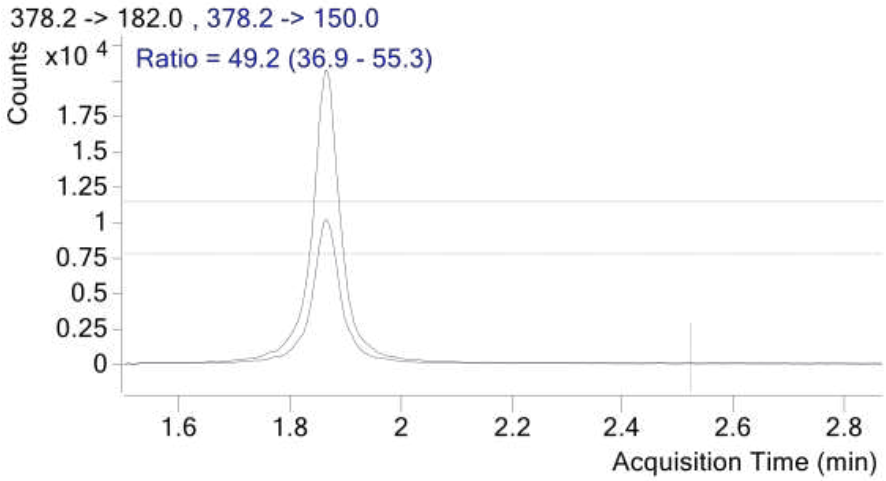

Figure 6.8. *Chromatogram of Pellet Exposed to DMSO for 8 Days: Conformation of TRA Presence*

Note. Figure 6.8(a) is the analysis of the TRA whereas Figure 6.8(b) is that of the internal standard. After 8 days of exposure to the pellet, no TRA was found in the pellet.

(a)

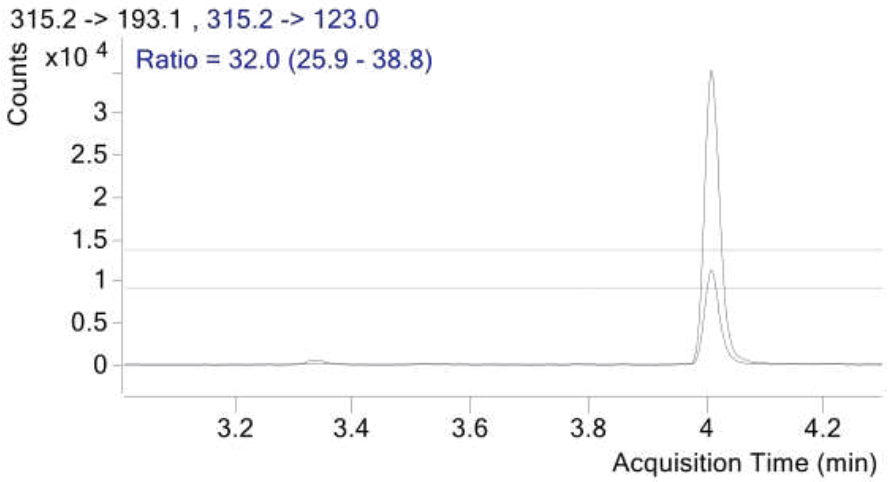

(b)

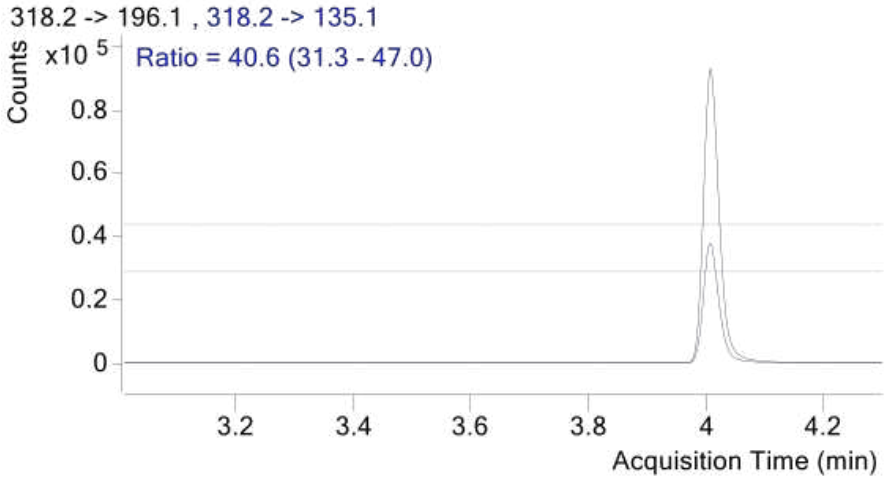

Figure 6.9. *Chromatogram of Pellet Exposed to 100 µM TRA and 10 µM CBD for 8 Days: Conformation of CBD Presence*

Note. Figure 6.9(a) is the analysis of the CBD whereas Figure 6.9(b) is that of the internal standard. One day of exposure to the pellet shows both the CBD and the internal standard in the pellet extraction.

(a)

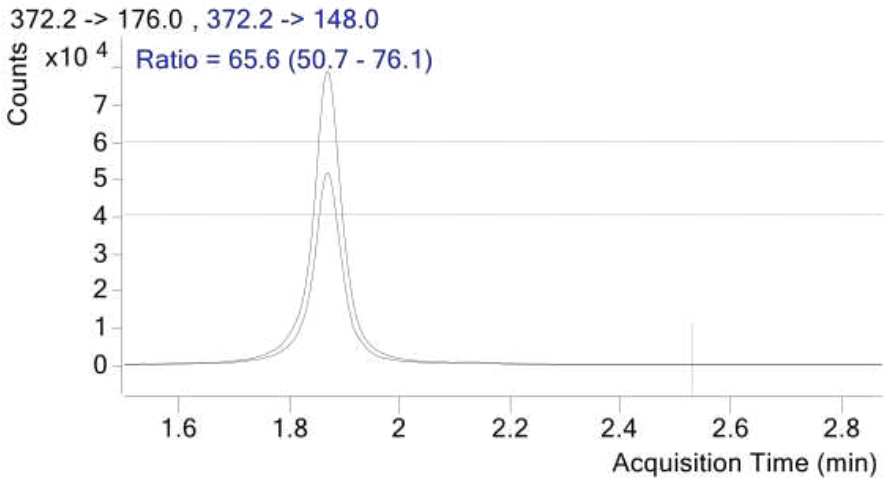

(b)

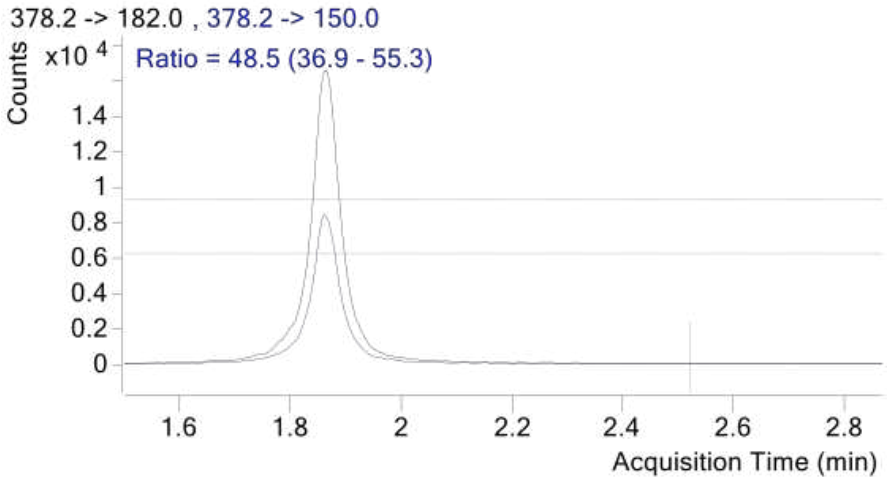

Figure 6.10. *Chromatogram of Pellet Exposed to 100 µM TRA and 10 µM CBD for 8 Days: Conformation of TRA Presence*

Note. Figure 6.10(a) is the analysis of TRA whereas Figure 6.10(b) is that of the internal standard. Eight days of exposure to the pellet shows both TRA and internal standard in the pellet extraction.

(a)

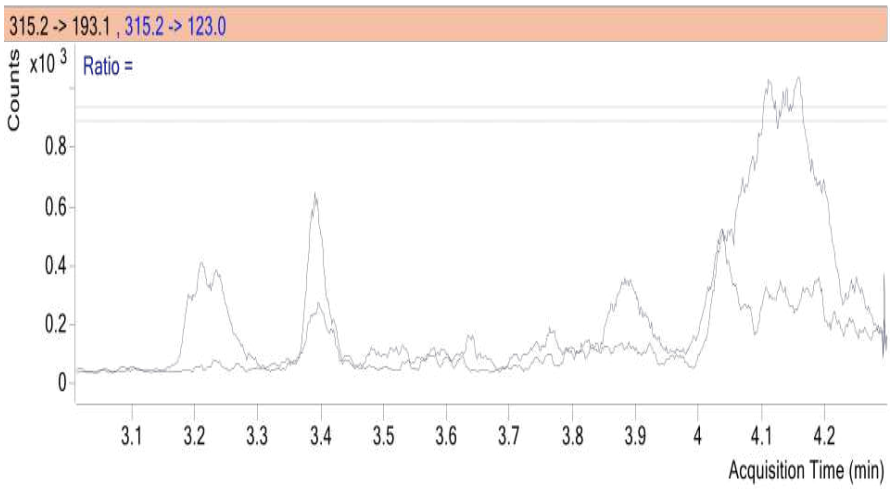

(b)

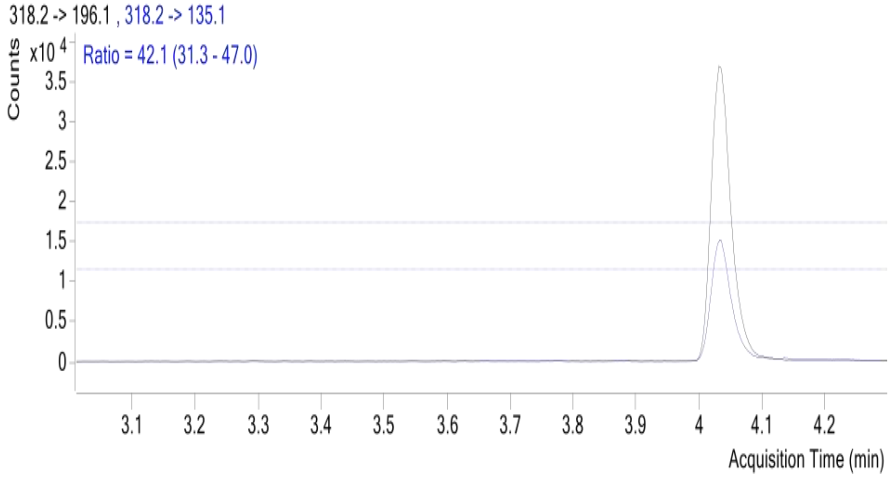

Figure 6.11. *Chromatogram of Wash Exposed to 100 µM TRA and 10 µM CBD for 8 Days: Conformation of CBD Presence*

Note. Figure 6.11(a) is the analysis of CBD whereas Figure 6.11(b) is that of the internal standard. Eight days of exposure to the pellet found no CBD in the wash, but the internal standard is present in the wash extraction.

(a)

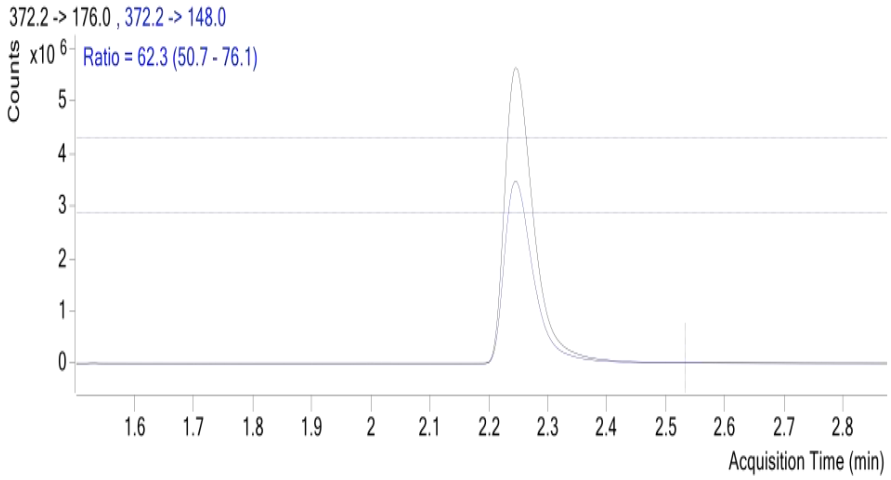

(b)

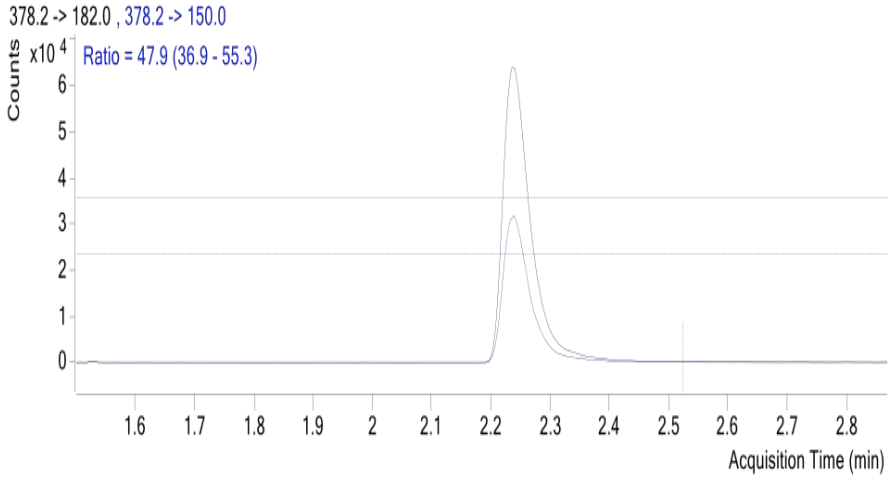

Figure 6.12. *Chromatogram of First Wash Exposed to 100 µM TRA and 10 µM CBD for 1 Day: Conformation of TRA Presence*

Note. Figure 6.12(a) is the analysis of TRA whereas Figure 6.12(b) is that of the internal standard. Eight days of exposure shows both TRA and internal standard in the wash extraction.

(a)

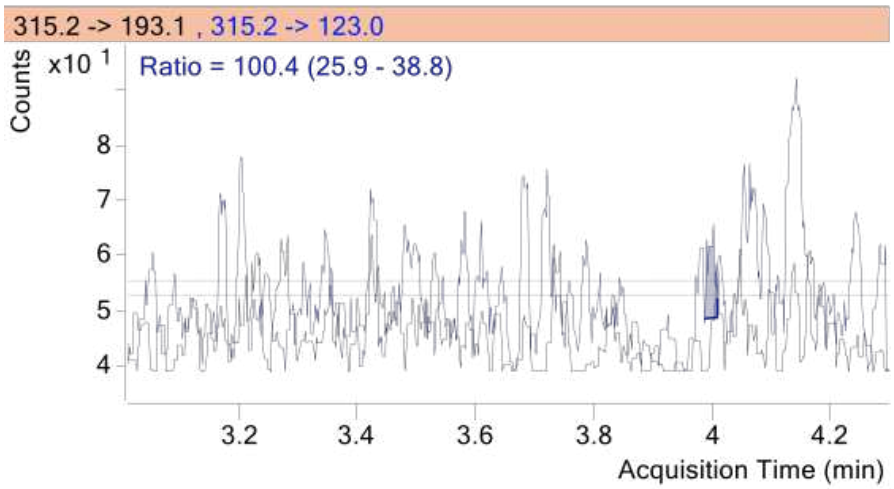

(b)

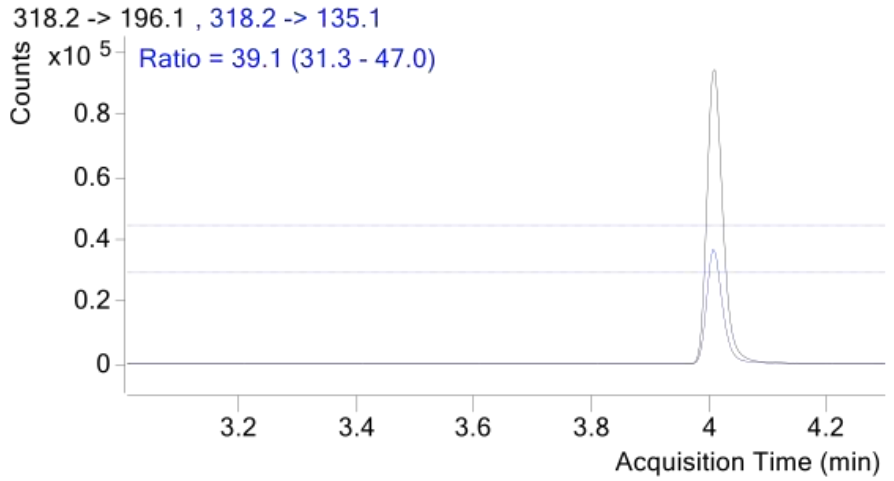

Figure 6.13. *Chromatogram of Pellet Exposed to DMSO for 16 Days: Conformation of CBD Presence*

Note. Figure 6.13(a) is the analysis of CBD whereas Figure 6.13(b) is that of the internal standard. Sixteen days of exposure to the pellet shows no CBD found in the pellet but the internal standard is present.

(a)

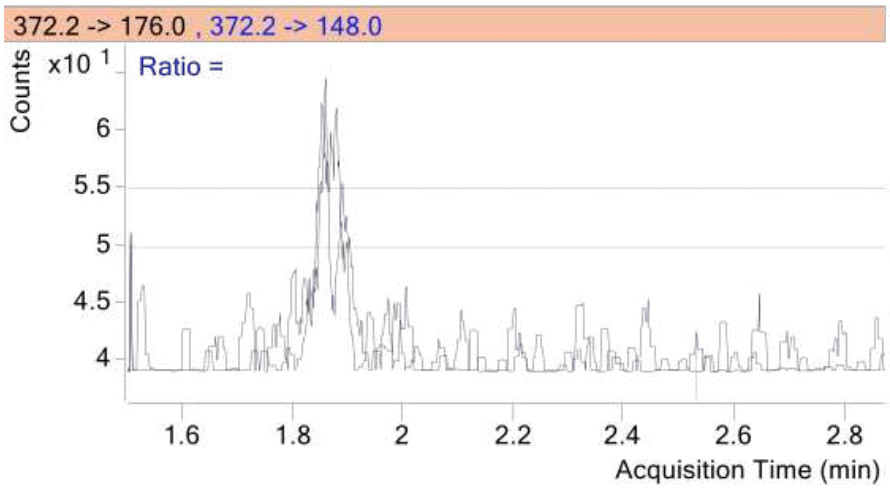

(b)

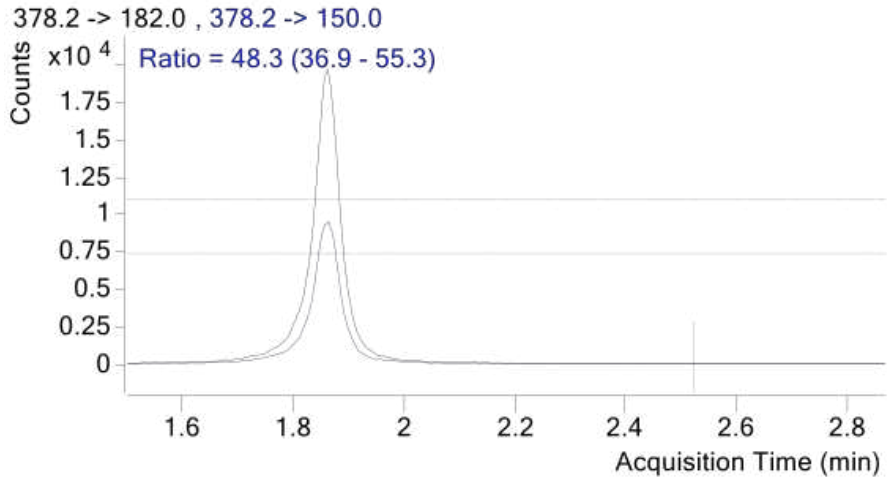

Figure 6.14. *Chromatogram of Pellet Exposed to DMSO for 16 Days: Conformation of TRA Presence*

Note. Figure 6.14(a) is the analysis of TRA whereas Figure 6.14(b) is that of the internal standard. Sixteen days of exposure to the pellet does not show TRA in the pellet, but the internal standard is present.

(a)

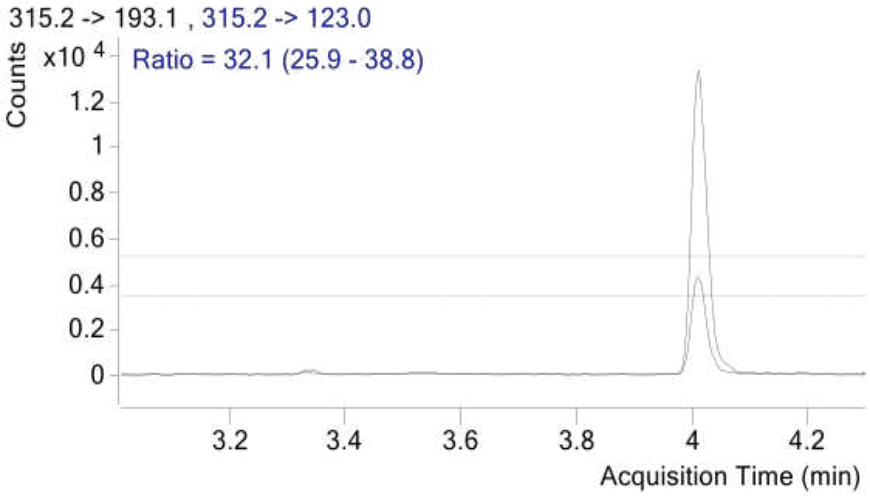

(b)

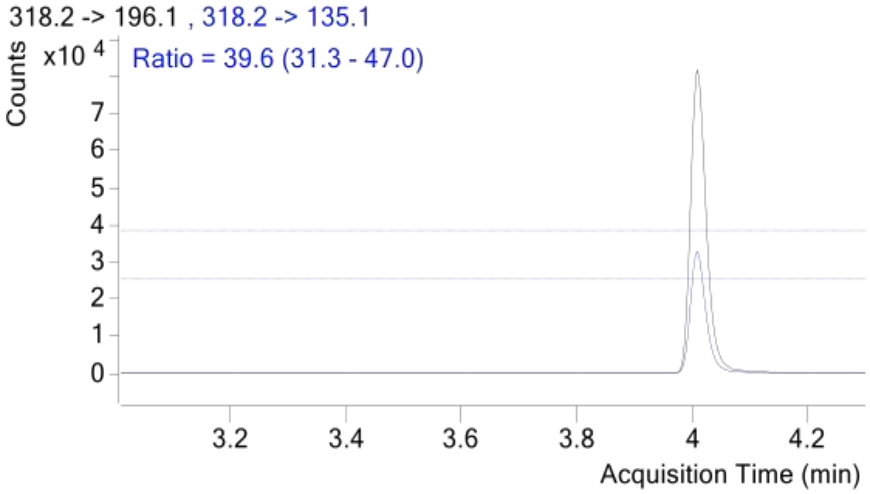

Figure 6.15. *Chromatogram of Pellet Exposed to 100 µM TRA and 10 µM CBD for 16 Days: Conformation of CBD Presence*

Note. Figure 6.15(a) is the analysis of CBD whereas Figure 6.15(b) is that of the internal standard. Sixteen days of exposure to the pellet shows both CBD and internal standard in the pellet extraction.

(a)

(b)

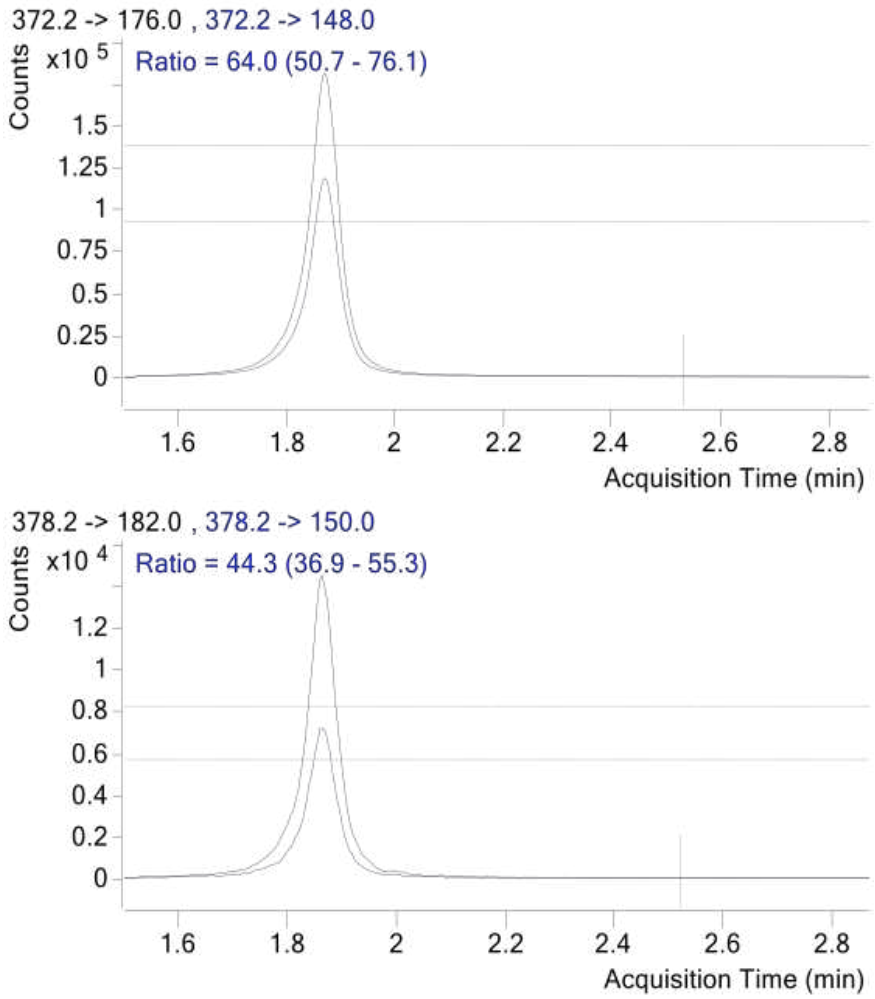

Figure 6.16. *Chromatogram of Pellet Exposed to 100 µM TRA and 10 µM CBD for 16 Days: Conformation of TRA Presence*

Note. Figure 6.16(a) is the analysis of TRA whereas Figure 6.16(b) is that of the internal standard. Sixteen days of exposure to the pellet shows both TRA and internal standard in the pellet extraction.

(a)

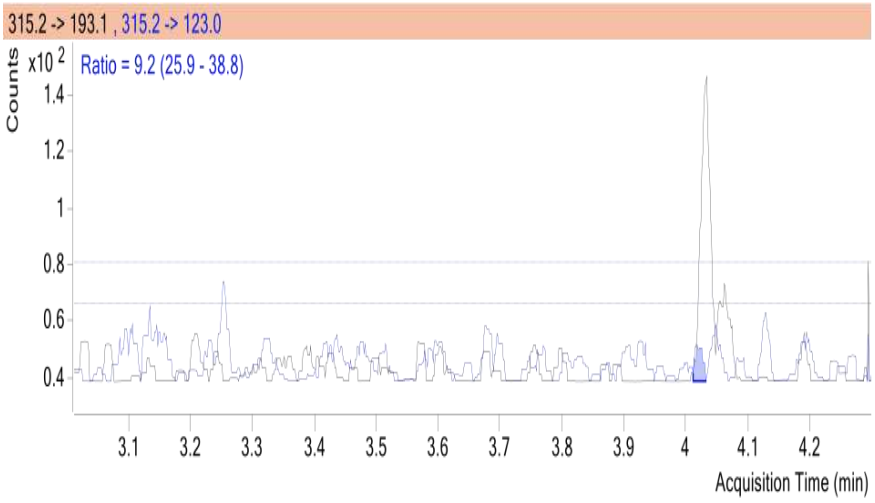

(b)

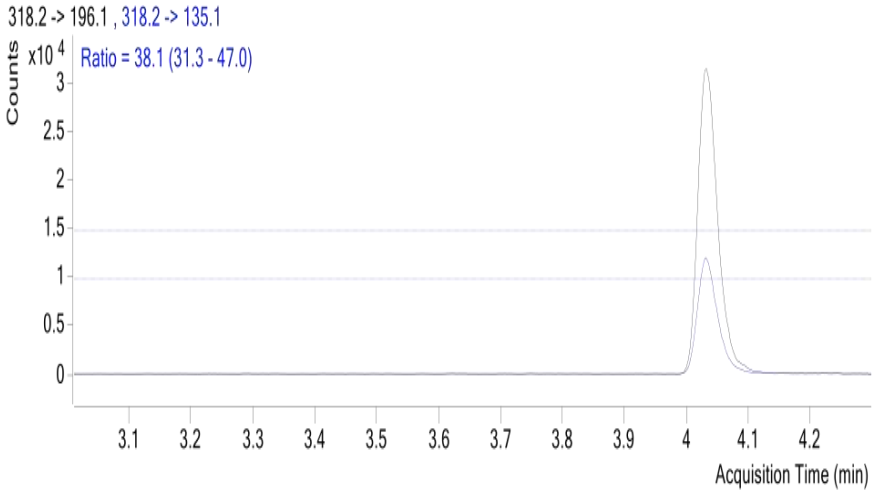

Figure 6.17. *Chromatogram of Wash Exposed to 100 µM TRA and 10 µM CBD for 16 Days: Conformation of CBD Presence*

Note. Figure 6.17(a) is the analysis of CBD whereas Figure 6.17(b) is that of the internal standard. Sixteen days of exposure to the pellet shows no CBD found in the wash but shows the internal standard is present.

(a)

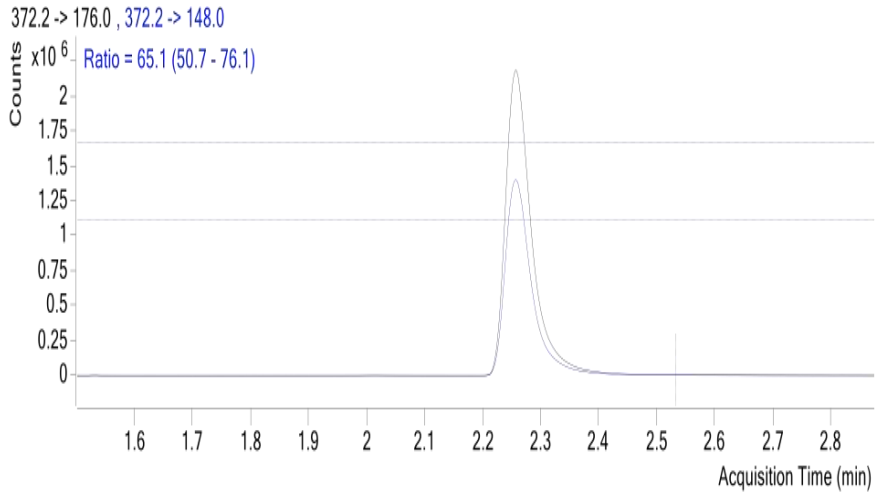

(b)

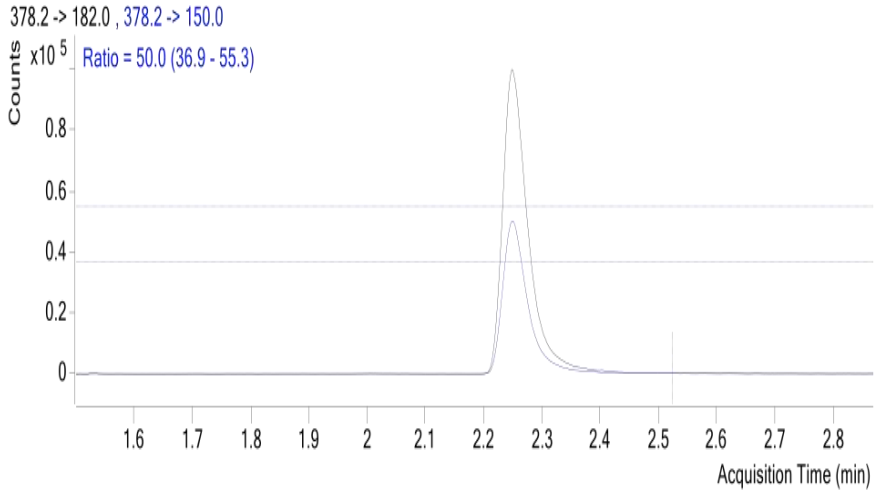

Figure 6.18. *Chromatogram of Wash Exposed to 100 µM TRA and 10 µM CBD for 16 Days: Conformation of TRA Presence*

Note. Figure 6.18(a) is the analysis of TRA whereas Figure 6.18(b) is that of the internal standard. After 16 days of exposure to the pellet, both TRA and the internal standard are found in the extraction.

(a)

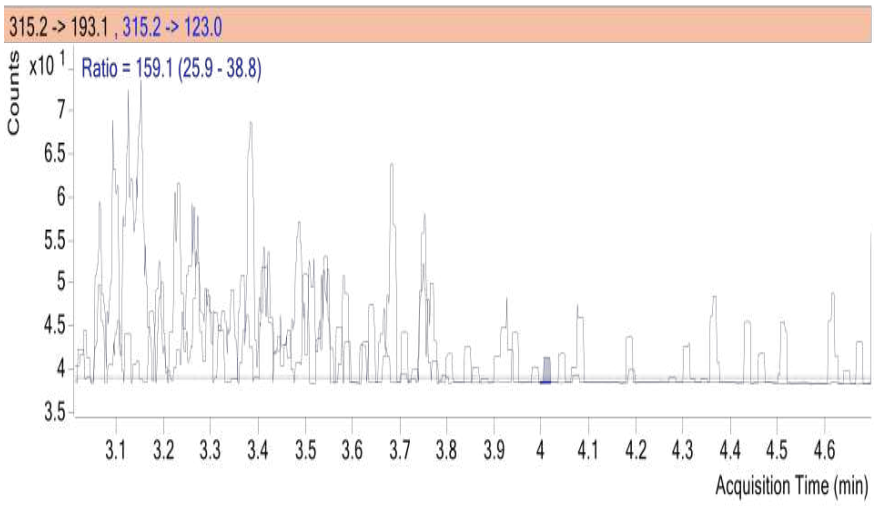

(b)

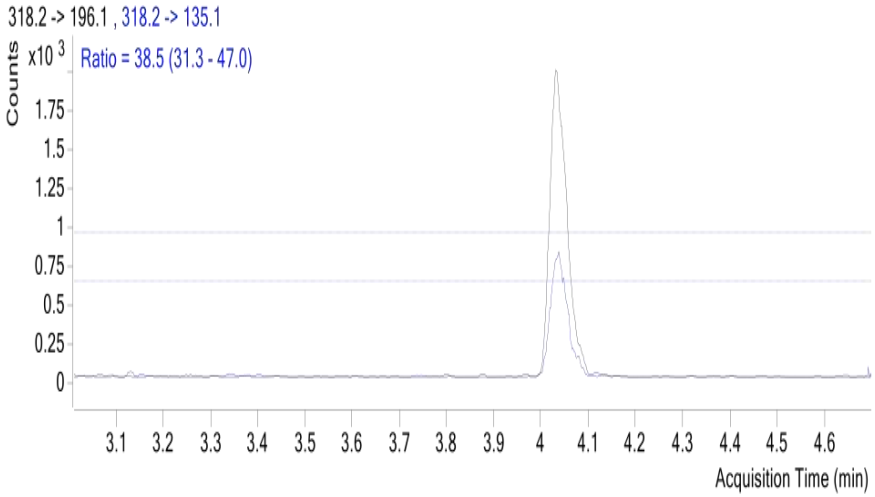

Figure 6.19. *Chromatogram of Pellet Exposed to 100 µM TRA and 10 µM CBD for 1 Day*: *Conformation of CBD Presence*

Note. This pellet, unlike those represented in the previous figures (Figs. 6.1–6.18), was centrifuged 25 times using PBS. Figure 6.19(a) is the analysis of CBD whereas Figure 6.19(b) is that of the internal standard. After 1 day of exposure, the pellet does not contain CBD but internal standard is present in the pellet extraction.

(a)

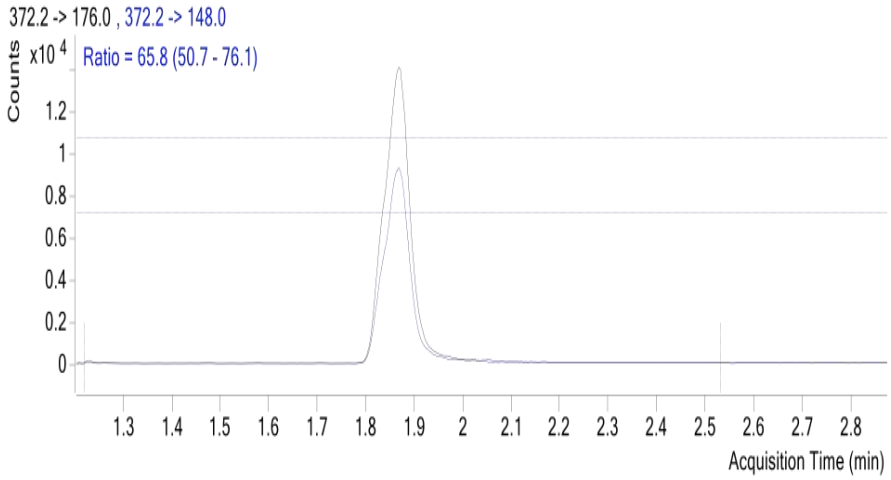

(b)

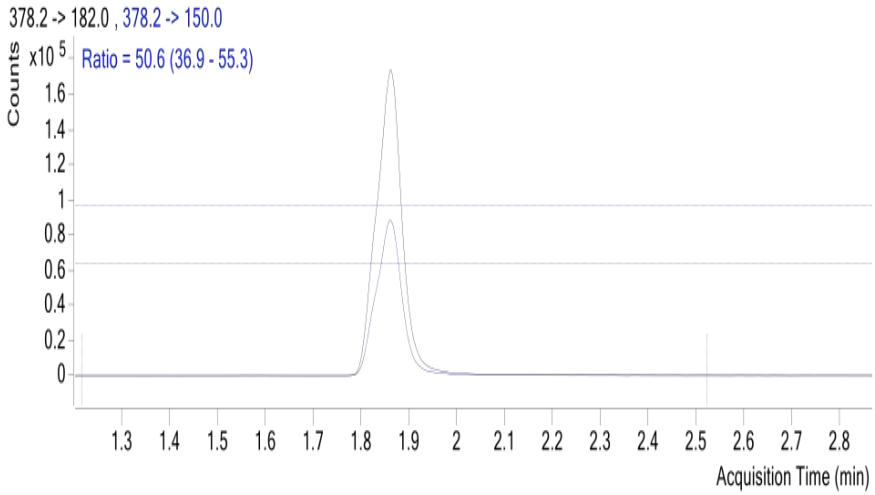

Figure 6.20. *Chromatogram of Pellet Exposed to 100 µM TRA and 10 µM CBD for 1 Day: Conformation of TRA Presence*

Note. This pellet, unlike those represented in Figures 6.1–6.18, was centrifuged 25 times using PBS. The pellet shows TRA found in the wash; the internal standard is also present.

(a)

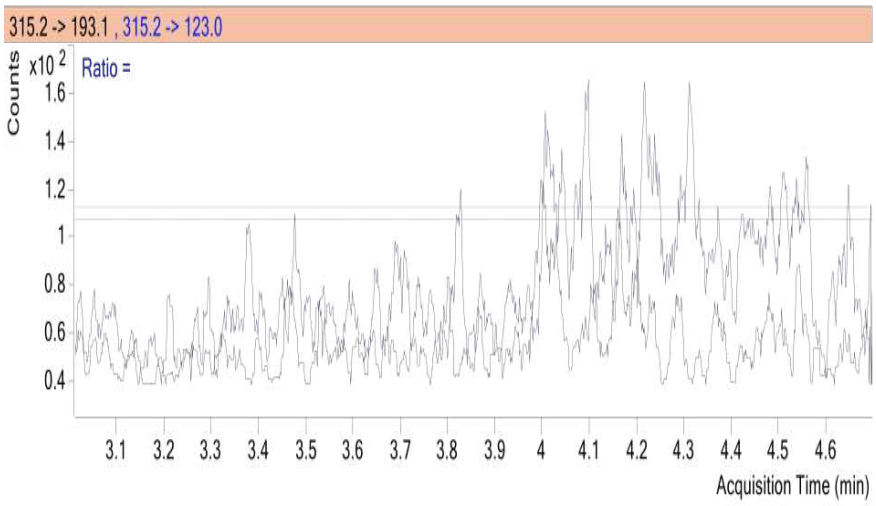

(b)

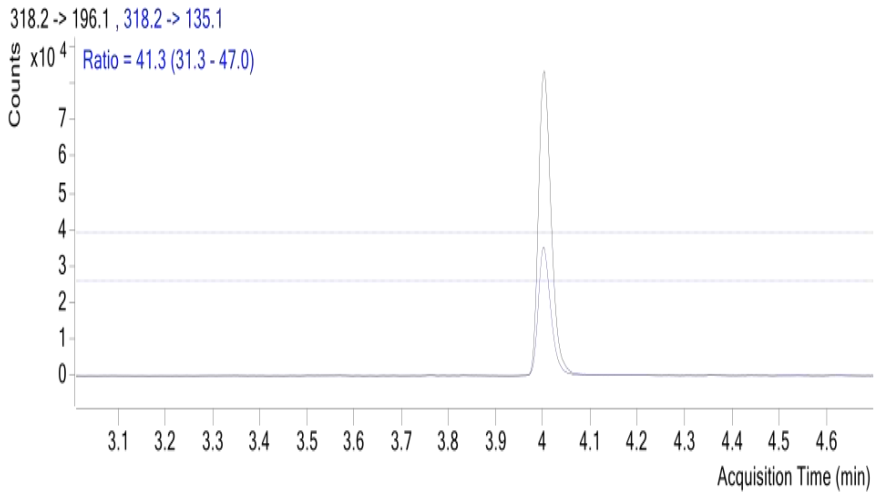

Figure 6.21. *Chromatogram of 1 mL Wash Centrifuged 25x From Exposure to 100 µM TRA and 10 µM CBD for 1 Day: Conformation of CBD Presence*

Note. Figure 6.21(a) is the analysis of CBD whereas Figure 6.21(b) is that of the internal standard. After 1 day of exposure, no CBD is found in the 25th wash but the internal standard is present.

(a)

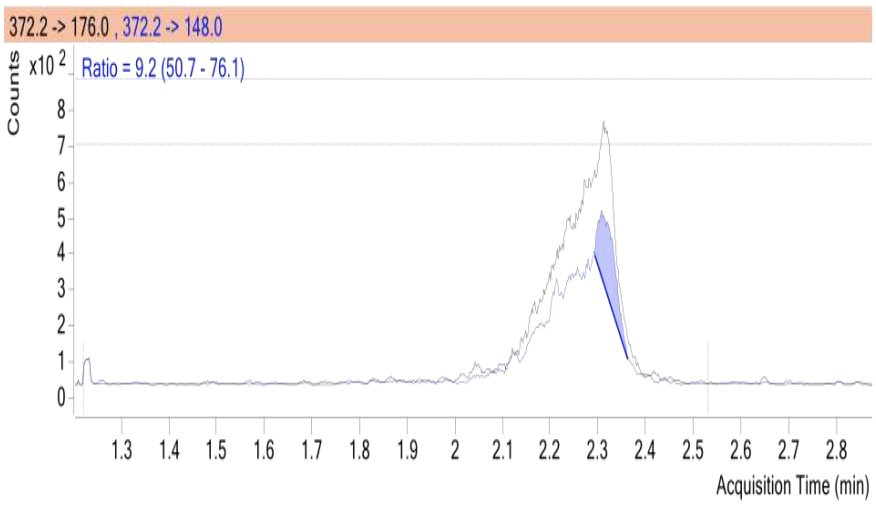

(b)

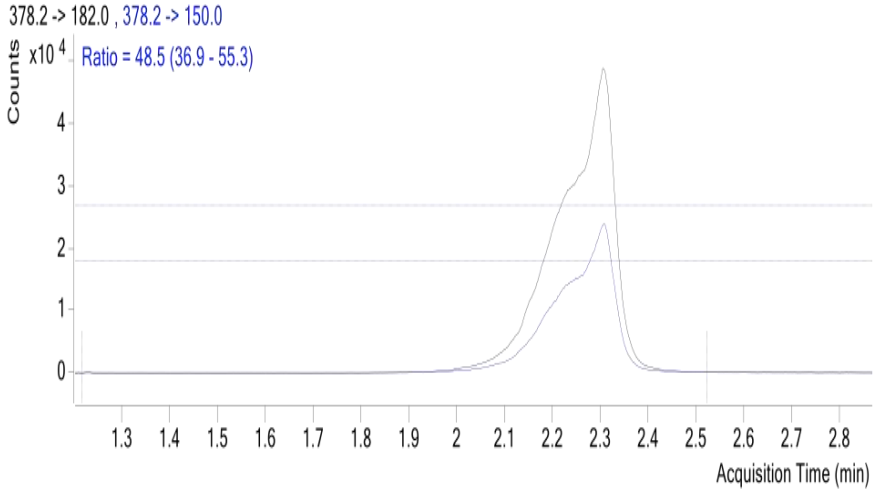

Figure 6.22. *Chromatogram of 1 mL 25th Wash From Exposure to 100 µM TRA and 10 µM CBD for 1 Day: Conformation of TRA Presence*

Note. Figure 6.22(a) is the analysis of TRA whereas Figure 6.22(b) is that of the internal standard. Because of errors in the extraction processes, resulting poor peak performance indicates it was not possible to confirm the presence of organic structures.

6.3 Results from LC-MS/MS on Internal Levels of CBD and TRA Conformation

It was hypothesized that increasing the washes would completely clear both TRA and CBD from the external side of the *C. elegans*, allowing for assessment of the internal levels of

both compounds. It was also hypothesized that not diluting the acetonitrile with water resulted in poor peak graphs shown in Figure 6.21. Also, the analysis of these washes was inconsistent as CBD was not present in the 25th pellet wash (see Fig. 6.22). We were not able to confirm the presence of organic structures in pellets because organic structures were identified in washes. Due to time constraints, it was not possible to optimize this protocol, but it is believed this could be a promising route in drug discovery and identification in nematode models.

CHAPTER 7

SUMMARY OF FINDINGS

7.1 Model Organism and Compounds of Interest

Alzheimer's disease has been characterized by the proliferation of both $A\beta_{1-42}$ and p-Tau within the brain (Ritchie et al., 2017). This disease currently has no cure and the strategy of previous therapeutics has been to directly target the $A\beta_{1-42}$ misfolded protein and increase the neurotransmitter acetylcholine ("Aducanumab (Aduhelm) for Alzheimer's disease," 2021; Birks & Harvey, 2018). In this study, we propose a therapeutic model that utilizes transgenic *C. elegans* as a model organism to investigate the role of a drug-stacking treatment with known compounds to target the eIF2-α-p and act as an ROS scavenger for AD (Halliday et al., 2017; Moreno et al., 2013; Tonnies & Trushina, 2017; Zhang et al., 2022). We hypothesized stacking two compounds with these characteristics would improve overall lifespan and quality of life for the nematodes. We found that both TRA and CBD in isolation increased lifespan (see Figs. 5.1–5.2).

The *C. elegans* models utilized for this study had either accumulated $A\beta_{1-42}$ or p-Tau. The first strain, Pro-Aβ Aggr., was engineered to express $A\beta_{1-42}$ by injecting human minigene $A\beta_{1-42}$ into the nematode to express $A\beta_{1-42}$ in the neurons (Fong et al., 2016). The second strain, Pro-Aβ Aggr., represented the control as it is genetically identical to our Wild Type, only differing by the presence of a YFP pharyngeal protein marker (Fong et al., 2016). The second neurodegenerative nematode, Pro-Tau Aggr., was engineered through a process of double-crossing two separate *C. elegans*, which had mutated K280 deletion and MAPT V337M (Fatouros et al., 2012). Both deletion of K280 and point mutation MAPT are crucial for the

formation of Tau mutation in this protein, which results in the misfolding of the protein and has been associated with neurodegenerative disorders (Spina et al., 2017; Strang et al., 2019). The culmination of these two deleterious genes results in the manifestation of p-Tau in the GABAeric motor neurons of our nematode model. The control strain used in our tau model was the Anti-Tau Aggr. *C. elegans* mutant, which was designed by double-crossing mutants resulting in a double knockout of K280 and V337M MAPT (Fatouros et al., 2012).

The two compounds we used for the drug-stacking treatment were trazadone and cannabidiol. TRA has been shown to target the UPR in neurodegenerative mice models by inhibiting the phosphorylation of the eIF2-α-p pathway (Halliday et al., 2017). We hypothesized from this evidence that targeting this pathway could ameliorate the lifespan and quality of life of AD-model *C. elegans* by targeting eIF2-α-p under chronic aggregation of both p-Tau and $A\beta_{1-42}$ (Halliday et al., 2017; Moreno et al., 2013; Mori, 2000). In a controlled trial looking at frontotemporal dementia patients supplemented with TRA, researchers found that the severity of symptoms in 50% of p-Tau-related patients decreased (Lebert et al., 2004). In addition, researchers have found that in neurodegenerative *C. elegans* with Tau-related disorders that TRA was a promising compound for motility of Tau mutants (Wood, 2017). The abundant data on the properties of TRA made it an excellent candidate for the purposes of our studies utilizing transgenic nematodes.

The second drug of interest, CBD, while mechanistically still not well-established, became a strong second candidate for use in drug-stacking treatments. The benefits of using CBD include, but are not limited to, the wide therapeutic index of the drug and the pre-existing receptors in the nematode model (Millar et al., 2019). In addition, the utilization of CBD previously has been administered to AD-modeled mice where the findings noted a reversal in

cognitive deficits (Cheng et al., 2014). The final piece of information we required to recruit this compound for our drug-stacking treatments was confirmation that *C. elegans* actually has the endogenous cannabinoid receptors 2-AG and AEA and that the literature establishes it as relatively non-toxic (Oakes et al., 2017). Additionally, CBD has been administered to *C. elegans* and both heat stress response and longevity were analyzed to deduce the efficacy in the observable toxicity of nematodes in the 0.4 µM to 4 mM range (Land et al., 2021). As previously mentioned, we believe that utilizing TRA and CBD in a drug-stacking therapy for neurodegenerative *C. elegans* could be promising due to the unique properties of TRA in targeting the UPR and of CBD as an ROS scavenger (Halliday et al., 2017; Zhang et al., 2022).

7.2 Determination of Dosages for Each Compound

In order to deduce what dosage(s) would be most effective for our nematode models, non-synchronous adults were subjected to a neuronal integrity test. The test was set up by having all strains of nematodes live on a plate that contained varying doses of TRA or CBD for 1 week. Following this 1-week exposure, adult nematodes were then touched using an eyelash on both the anterior and posterior dorsal sides. A normal, healthy response would represent itself as the nematode's ability to flee from both stimuli. The forward fleeing and backward fleeing family of interneurons had repeated touches due to research citing multiple touches and observing movement as a better way to observe neuronal integrity (McClanahan et al., 2017). Fleeing from both stimuli was regarded as a 100% response. If the nematodes only fled from one or neither stimuli the response was recorded as 0%. From this assay we discovered that for our AD-modeled strains, the most promising dosages of TRA were 100 µM and 200 µM (see Fig. 4.1, Panels A and B). For CBD, the most promising doses were 5 µM and 10 µM (see Fig. 4.1, Panel

C). The finding regarding the dose of 10 µM is confirmed by the findings of Land et al. (2021), in relation to extending the lifespan of *C. elegans*.

Once we deduced the two most promising doses for each drug, we then created NGM agar plates which had both 100 µM TRA and 10 µM CBD. Regarding the timing of treatment, we referenced the paper from the engineers of the $A\beta_{1-42}$ as a guideline for time of exposure (Fong et al., 2016). According to the researchers, they noted that the nematodes are middle-aged on Day 8, and with western blot data, peak concentration of the misfolded protein aggregation occurs on Day 12 (Fong et al., 2016). To obtain a complete picture of treatment, we treated nematodes on Day 1 and repeated the touch test on Day 7; treated nematodes on Day 8 and repeated the touch test on Day 12; and then treated on Day 16 and repeated the touch test on Day 18 (see Fig. 4.6). By spreading out the times of treatment, we were able to analyze full-life, middle-age, and late-stage rescue.

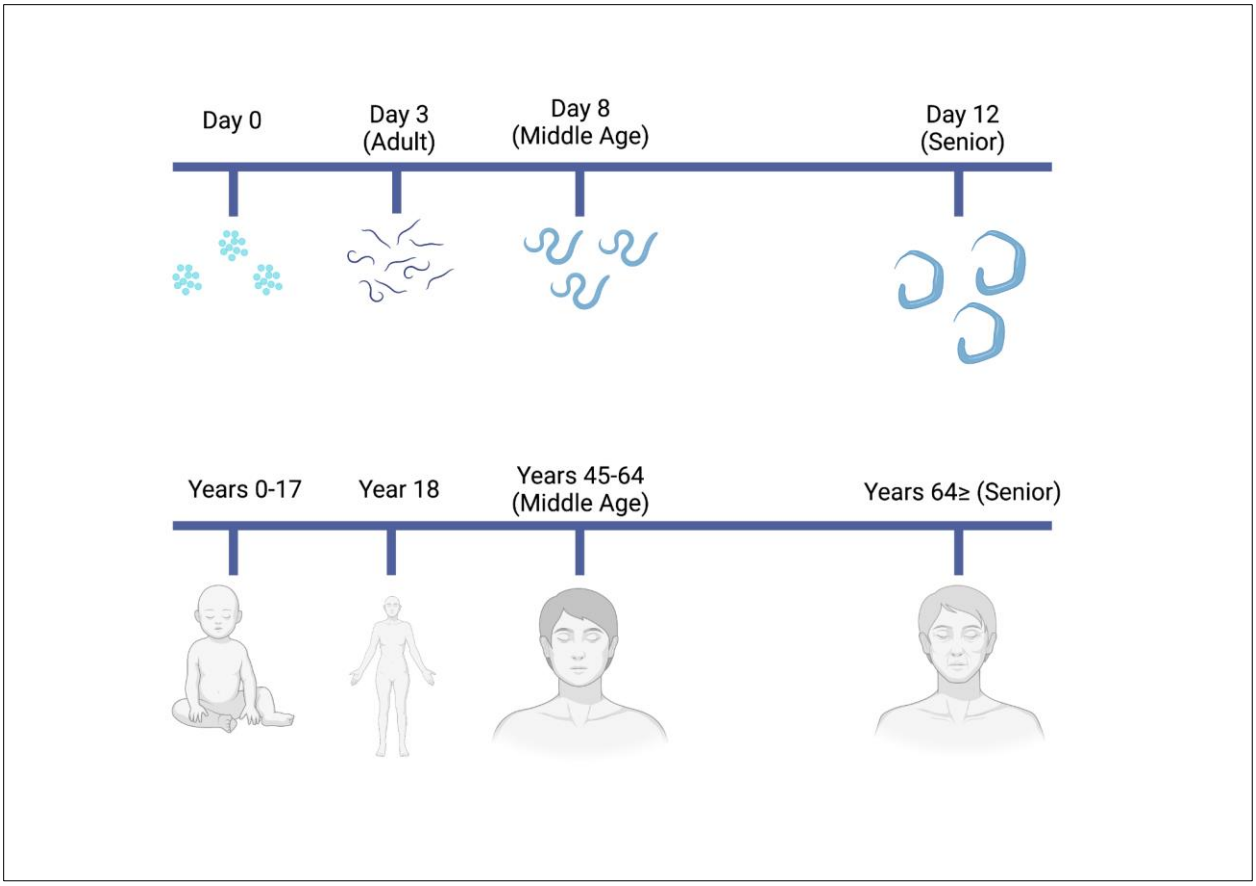

Figure 7.1. *CDC-Developed Lifespan Comparison: Pro-Aβ Aggr. and Human Being*

Note. This figure depicts the parallel stages of aging between Gru102 *C. elegans* (Pro-Aβ Aggr.) and a human being. Developed using information from Fong et al. (2016). Image created by author using BioRender.

With full-life exposure to the combination of treatments, all of our control and experimental models were not significantly changed compared to vehicle treatment at Day 7 (see Figs. 4.2–4.5). We hypothesize this is due to the fact that the aggregation of these proteins had not reached a point where it was deleterious to the nematodes (Brignull et al., 2007). This is again supported by the engineers of the $A\beta_{1\text{-}42}$, who state there are no phenotypic changes seen until Day 8 (Fong et al., 2016). However, at both mid-life and late-stage, we began to see

promising results. Our data suggests that neuronal integrity is improved in Pro-Aβ Aggr. and Pro-Tau Aggr. strains by our drugs of interest (see Figs. 4.1 and 4.6). For our control strains, the touch test employed on both Day 12 and Day 18 showed no significant effect (see Fig. 4.6). However, for both Pro-Tau Aggr. and Pro-Aβ Aggr., there were significant effects to motility response on both Day 12 and Day 18 touch tests for our treatments when compared to vehicle (see Fig. 4.6). While the experimental models did not reach the response level seen in control strains, this was encouraging data that pointed to the combination of TRA and CBD being an effective agent regarding neuronal integrity as represented by motility response.

7.3 Analysis of Longevity Assay

Due to the short lifespan of the nematodes and the previously mentioned days of interest, we utilized 96-well Microtiter plates to analyze the lifespans in the presence of the compounds (Cornwell & Samuelson, 2020; Fong et al., 2016; Solis & Petrascheck, 2011; Urban et al., 2021). While there are some notable limitations involved in utilizing nematodes in a survival analysis as compared to other mammals—due to their less complex anatomy—utilizing this assay proved advantageous for deducing beneficial concentrations of each drug (Wang et al., 2019). As discussed in Section 3.4.2, for this assay we first synchronized nematodes utilizing a bleach and sodium hydroxide solution and the following day plated the nematodes in the 96-well plate. We again used full-life, middle-age, and late-stage rescue days as a benchmark for accessing the potential benefits of the compounds. It should be noted that the drug Floxuridine (FUdR) was given at 50 μM on Day 3 due to its ability to inhibit the progenerating of nematodes so we could be assured that the nematodes counted were not new ones that potentially hatched in the well (Park et al., 2017; Solis & Petrascheck, 2011). Furthermore, FUdR has been found to extend nematode lifespan and researchers should be diligent when analyzing compounds for age

extension that the effect is from the compounds of interest and not from Floxuridine (Wang et al., 2019). To ensure what was being analyzed was not due to FUdR, all vehicle treatments were also treated with 50 µM FUdR. In this project, we first wanted to observe how the individual drugs acted on the nematodes. We investigated TRA at 25 µM, 50 µM, and 100 µM concentrations, whereas with CBD we investigated 1 µM, 5 µM, and 10 µM. Dosages used to improve neuronal integrity also improved lifespan in multiple models of *C. elegans*. Surprisingly, our Anti-Tau Aggr. control model showed significantly improved lifespan at higher doses of 10 µM CBD and 25 µM, 50 µM, and 100 µM TRA (see Fig. 5.1). One factor that might have contributed to this is that knocking out MAPT may result in some deleterious effects on both motility and musculature integrity (Goncalves et al., 2020). It seems that for late stage rescue, the dose of CBD needs to be increased up to 10 µM and TRA increased to 100 µM (see Fig. 5.2). This is to be expected due to the nature of the accumulation of the misfolded proteins and the degradation of cellular stress that follows (Chaudhuri & Paul, 2006). We are currently working on both repeating this experiment and implementing triplicate studies analyzing the combination of 10 µM CBD and 100 µM TRA at the same time points for lifespan analysis.

7.4 Immunofluorescence

One of the questions relating to AD is whether the misfolding of proteins is responsible for or a symptom of the disease. To attempt to answer this question, we utilized the nematodes from the touch test and stained them with various protein markers, using two separate antibodies—one for p-tau and one for $A\beta_{1-42}$. To have confirmation that this assay worked, we utilized DAPI as a morphological marker. The first antibody we used was AT270 (ThermoFisher), a phospho-Tau marker that was analyzed at Threonine 181, site of the amino acid sequence (Lewczuk et al., 2004). The second marker used was beta-Amyloid (1-42)

polyclonal antibody (ThermoFisher), which marked the 36-42 C-terminal region that has also been associated with AD (Citron et al., 1996).

To tag the nematodes, we first used a technique called "snap freeze" to break the chitin, a hard shell surrounding their bodies that antibodies cannot penetrate unless it is broken. Chitin also makes nematode bodies resistant to staining (Duerr, 2013). For AT270 we used a 1:2000 ratio, for the beta-Amyloid (1-42) polyclonal antibody we used a 1:400 ratio, and for DAPI we used a 1:2000 ratio. Both antibodies were left on the nematodes overnight at 4 °C. The worms were stained with DAPI for 3 min at room temperature.

7.5 Limitations

This research was geared toward drug-stacking treatments with known UPR pathway agonists and ROS scavengers on AD-model organisms (Halliday et al., 2017; Moreno et al., 2013; Zhang et al., 2022). It should be noted that the models we used only expressed one of the two aforementioned misfolded proteins. While there are homologs presented in *C. elegans*, nematodes as a whole are not the best representations for mammals afflicted with the disease due to their simple anatomy (Tissenbaum, 2015). Another potential limitation is the mixed response to the Pro-Tau Aggr. strain and its specific mutations—K280 deletion and MAPT V337M—have been associated with frontal temporal dementia, which can be misdiagnosed as AD (Spina et al., 2017). As far as the experimental design, one limitation is related to the immunofluorescence assay. This issue is related to the potential that the *C. elegans* can be damaged when the method of freezing the nematodes and cracking them open is employed. There is a possibility that structures can be damaged if the protocol is done incorrectly and therefore the method might not obtain the best representation of the proteins present (Duerr, 2013).

Our investigations utilizing LC-MS/MS did not confirm the presence of organic structures inside the nematode pellet because of the presence of organic structures in the washes. It is hypothesized that this is both due to the size of the pellets and the concentrations used for the treatments. Most pellets for all exposure dates were extremely small, weighing no more than 0.4 mg/15 mL. Adding centrifugation and washing decreased the overall size of the pellet. Literature regarding optimal tissue sample size indicate a minimum of 1 mg/mL (Wilson et al., 2010). Moreover, even only 10 µM of CBD and 100 µM TRA took approximately 25 centrifugation washes to completely clear (see Figs. 6.21–6.22). However, while TRA was found in the pellet, CBD was not (see Fig. 6.19).

Finally, one of the biggest limitations is related to the timing of treatment of the Pro-Tau Aggr. strain, because the times at which the nematodes were dosed were based on the aging process of the $A\beta_{1-42}$ strain rather than a specifically established one for the Tau model (Fong et al., 2016). Because of this, our experimental model may have been optimized for our Pro-Aβ Aggr strain but not our Pro-Tau Aggr. strain.

7.6 Future Studies

Currently, we are working on producing longevity data with combinational treatments of 10 µM CBD and 100 µM TRA. We are also collecting triplicate IFA results from combinational treatments to assess the various timepoints of treatment and accumulation of misfolded proteins. The mechanism of how CBD works is not well-established. It has been shown that CBD has been implicated to act on Nrf-2, activating the antioxidant response element (ARE) and inhibiting NF-kB through $PPAR_{\gamma}$ (Esposito et al., 2011; O'Sullivan, 2016). One of our goals is to deduce the potential pathway of CBD by acquiring mutant *C. elegans* that are hypomorphic for Nrf-2. We will deduce if CBD acts independently as an ROS scavenger or activates Nrf-2

following UV exposure. To implement this study, we recruited the ID1 mutant *C. elegans* strain, which is genetically engineered to roll in the presence of oxidative stress and glow green due to its Nrf-2 homolog, Skn-1, being activated (Wang et al., 2013). We believe that by implementing this model it will be possible to deduce both potential Nrf-2 activation in the presence of CBD and potential benefits of the drug to the organism when exposed to a stressor. This mutant nematode has been tagged with a GFP marker for its Nrf-2 homolog and we can therefore use fluorescence microscopy to qualitatively see how different treatments of both induction of ROS and CBD activate this pathway. Another way we intend to measure the presence of ROS in these mutant *C. elegans* is to incorporate Dihydroethidium (Thermo Fisher Scientific), a fluorescent dye that measures levels of ROS via a spectrophotometer (Maremonti et al., 2020)

Another future direction would be to utilize a higher order animal model. We believe that canines would be a promising model of study, not only because of their increased complexity when compared to nematodes, but also because they contain certain pathways that nematodes do not, for example NF-kB. In addition to the similarities in canine development of neurodegeneration, there is a large body of evidence showing both the efficacy and pharmacodynamics of the two drugs we studied in canines. CBD is both very safe and cited as most beneficial through dermal treatment utilizing LC-MS/MS (Bartner et al., 2018). Furthermore, TRA has a long history of veterinary use and PKPD values have also been established (Jay et al., 2013). Moving toward higher order mammals would also be beneficial for this research due to the close similarities of human and canine cognitive dysfunction. Additionally the established doses and route of treatment for each compound in canines would require less optimization. The behavioral and longevity protocols to study the combination of

TRA and CBD would be both longer and much more complex, but would ultimately prove to be more translationally relevant.

7.7 Conclusions

We hypothesized that treatments of compounds known to both target the UPR and scavenge ROS would ameliorate *C. elegans* that expressed either p-Tau or $A\beta_{1\text{-}42}$. To study these potentially beneficial effects of our drugs of interest, we examined a multitude of studies that measured neuronal integrity and longevity. We recruited two drugs that have been implicated to improve the overall quality of life in multiple models of Alzheimer's disease.

This study assessed the utilization of TRA and CBD in the AD nematode models that expressed $A\beta_{1\text{-}42}$ or p-Tau. Our data support that both middle-aged and late-stage rescue utilizing doses of 10 µM CBD and 100 µM TRA significantly improved the neuronal integrity of the nematodes as assessed with a touch test assay (see Fig. 4.6). Doses of 5 µM and 10 µM of CBD and 25 µM, 50 µM, and 100 µM of TRA in isolation elongated the lifespan of our neurodegenerative *C. elegans* (see Figs. 5.1–5.2). Based on the survival analysis and neuronal integrity assay (see Fig. 4.6) both isolated treatments and combinational treatments of known URP-targeting and ROS-scavenging compounds may prove a unique avenue for treating Alzheimer's disease.

C. elegans differs from humans in many ways, however, it remains a beneficial model to study due to its shortened lifespan, homology to certain proteins, and fully mapped out connectome. From our work with the nematodes, we now have a better understanding of how both CBD and TRA affect the neuronal integrity and longevity of the animals at varying stages of life and times of exposure. Unlike previous publications studying Alzheimer's modeled *C. elegans*, which looked at only one or the other of the two proteins of interest, our study included

both p-Tau and $A\beta_{1-42}$. These findings obtained by researching nematodes can ideally be further implemented translationally in other models of Alzheimer's disease.

REFERENCES

Aducanumab (Aduhelm) for Alzheimer's disease. (2021). *The Medical Letter on Drugs and Therapeutics, 63*(1628), 105–106. https://www.ncbi.nlm.nih.gov/pubmed/34543258

Agnoli, A. (1986, October). Historique et pharmacologie de la trazadone [History and pharmacology of trazodone]. *Encephale*, *12*, 239–242. https://www.ncbi.nlm.nih.gov/pubmed/2880711

Alonso-Zaldivar, R. (2022, January 11). Medicare limits coverage of $28,000-a-year Alzheimer's drug. *Los Angeles Times*. https://www.latimes.com/business/story/2022-01-11/medicare-limits-coverage-of-28000-a-year-alzheimers-drug

Bakas, T., van Nieuwenhuijzen, P. S., Devenish, S. O., McGregor, I. S., Arnold, J. C., & Chebib, M. (2017). The direct actions of cannabidiol and 2-arachidonoyl glycerol at $GABA_A$ receptors. *Pharmacological Research*, *119*, 358–370. https://doi.org/10.1016/j.phrs.2017.02.022

Bartels, C., Wagner, M., Wolfsgruber, S., Ehrenreich, H., Schneider, & A. (2018). Impact of SSRI therapy on risk of conversion from mild cognitive impairment to Alzheimer's dementia in individuals with previous depression. *The American Journal of Psychiatry*, *175*(3), 232–241. Alzheimer's Disease Neuroimaging Initiative. https://doi.org/10.1176/appi.ajp.2017.17040404

Bartner, L. R., McGrath, S., Rao, S., Hyatt, L. K., & Wittenburg, L. A. (2018). Pharmokinetics of cannabidiol administered by 3 delivery methods at 2 different dosages to healthy dogs. *Candian Journal of Veterinary Research*, *82*(3), 178–184. https://pubmed.ncbi.nlm.nih.gov/30026641/

Birks, J. S., & Harvey, R. J. (2018, June 18). Donepezil for dementia due to Alzheimer's disease. *Cochrane Database of Systematic Reviews, 6*, CD001190. https://doi.org/10.1002/14651858.CD001190.pub3

Bisogno, T., Hanus, L., De Petrocellis, L., Tchilibon, S., Ponde, D. E., Brandi, I., Moriello, A. S., Davis, J. B., Mechoulam, R., & Di Marzo, V. (2001). Molecular targets for cannabidiol and its synthetic analogues: Effect on vanilloid VR1 receptors and on the cellular uptake and enzymatic hydrolysis of anandamide. *British Journal of Pharmacology, 134*(4), 845–852. https://doi.org/10.1038/sj.bjp.0704327

Bloom, G. S. (2014). Amyloid-β and tau: The trigger and bullet in Alzheimer disease pathogenesis. *JAMA Neurology*, *71*(4), 505–508. https://doi.org/10.1001/jamaneurol.2013.5847

Brenner, S. (1974). The genetics of *Caenorhabditis elegans*. *Genetics, 77*(1), 71–94. https://doi.org/10.1093/genetics/77.1.71

Brignull, H. R., Morley, J. F., & Morimoto, R. I. (2007). The stress of misfolded proteins: *C. elegans* models for neurodegenerative disease and aging. In P. Csermely & L. Vígh (Eds.) Molecular aspects of the stress response: Chaperones, membranes and networks (pp. 167–189). Springer. https://doi.org/10.1007/978-0-387-39975-1_15

Cabreiro, F., Au, C., Leung, K. Y., Vergara-Irigaray, N., Cochemé, H. M., Noori, T., Weinkove, D., Schuster, E., Greene, N. D. E., & Gems, D. (2013). Metformin retards aging in *C. elegans* by altering microbial folate and methionine metabolism. *Cell, 153*(1), 228–239. https://doi.org/10.1016/j.cell.2013.02.035

Centers for Disease Control and Prevention. (2020). *What is Alzheimer's disease?* U.S. Department of Health and Human Services. https://www.cdc.gov/aging/aginginfo/alzheimers.htm

Chakrapani, B. P. S., Kumar, S., & Subramaniam, J. (2008). Development and evaluation of an *in vivo* assay in *Caenorhabditis elgans* for screening compounds for their effect on cytochrome P_{450} expression. *Journal of Biosciences*, *33*(2), 269–277. https://doi.org/10.1007/s12038-008-0044-5

Chaudhuri, T. K., & Paul, S. (2006). Protein-misfolding diseases and chaperone-based therapeutic approaches. *The FEBS Journal, 273*(7), 1331–1349. https://doi.org/10.1111/j.1742-4658.2006.05181.x

Cheng, D., Spiro, A. S., Jenner, A. M., Garner, B., & Karl, T. (2014). Long-term cannabidiol treatment prevents the development of social recognition memory deficits in Alzheimer's disease transgenic mice. *Journal of Alzheimer's Disease, 42*(4), 1383–1396. https://doi.org/10.3233/JAD-140921

Citron, M., Diehl, T. S., Gordon, G., Biere, A. L., Seubert, P., & Selkoe, D. J. (1996). Evidence that the 42- and 40-amino acid forms of amyloid β protein are generated from the β-amyloid precursor protein by different protease activities. *Proceedings of the National Academy of Sciences of the United States of America, 93*(23), 13170–13175. https://doi.org/10.1073/pnas.93.23.13170

Clark, P. L. (2004). Protein folding in the cell: Reshaping the folding funnel. *Trends in Biochemical Sciences*, 29(10), 527–534. https://doi.org/10.1016/j.tibs.2004.08.008

Colovic, M. B., Krstic, D. Z., Lazarevic-Pasti, T. D., Bondzic, A. M., & Vasic, V. M. (2013). Acetylcholinesterase inhibitors: Pharmacology and toxicology. *Current Neuropharmacology, 11*(3), 315–335. https://doi.org/10.2174/1570159X11311030006

Cornwell, A. B., & Samuelson, A. V. (2020). Analysis of lifespan in *C. elegans*: Low- and high-throughput approaches. In S. Curran (Ed.), *Methods in molecular biology* (Vol. 2144, pp. 7–27). Humana. https://doi.org/10.1007/978-1-0716-0592-9_2

Cummings, J. L., Geldmacher, D., Farlow, M., Sabbagh, M., Christensen, D., & Betz, P. (2013). High-dose donepezil (23 mg/day) for the treatment of moderate and severe Alzheimer's disease: Drug profile and clinical guidelines. *CNS Neuroscience & Therapeutics*, *19*(5), 294–301. https://doi.org/10.1111/cns.12076

Duerr, J. S. (2013). Antibody staining in *C. elegans* using "freeze-cracking". *JoVE Journal*, (80), e50664. https://doi.org/10.3791/50664

Eisenmann, D. M. (2005). Wnt signaling. In H. Sawa & H. C. Korswagen (Eds.), *WormBook: The online review of* C. elegans *biology*. https://doi.org/10.1895/wormbook.1.7.1

Esposito, G., Scuderi, C., Valenza, M., Togna, G. I., Latina, V., De Filippis, D., Cipriano, M., Carratu, M. R., Iuvone, T., & Steardo, L. (2011). Cannabidiol reduces Aβ -induced neuroinflammation and promotes hippocampal neurogenesis through PPARγ involvement. *PLoS One, 6*(12), e28668. https://doi.org/10.1371/journal.pone.0028668

Fatouros, C., Pir, G. J., Biernat, J., Koushika, S. P., Mandelkow, E., Mandelkow, E. M., Schmidt, E., & Baumeister, R. (2012). Inhibition of tau aggregation in a novel *Caenorhabditis elegans* model of tauopathy mitigates proteotoxicity. *Human Molecular Genetics*, *21*(16), 3587–3603. https://doi.org/10.1093/hmg/dds190

Fong, S., Teo, E., Ng, L. F., Chen, C. B., Lakshmanan, L. N., Tsoi, S. Y., Moore, P. K., Inoue, T., Halliwell, B., & Gruber, J. (2016). Energy crisis precedes global metabolic failure in a novel *Caenorhabditis elegans* Alzheimer disease model. *Scientific Reports*, *6*, 33781. https://doi.org/10.1038/srep33781

Goncalves, R. A., Wijesekara, N., Fraser, P. E., & De Felice, F. G. (2020). Behavioral abnormalities in knockout and humanized tau mice. *Frontiers in Endocrinology, 11*, 124. https://doi.org/10.3389/fendo.2020.00124

Goodwin, K. (2021, June 18). Rival drugs of Biogen's Aduhelm may help prove FDA's highly criticized approval. *BioSpace*. https://www.biospace.com/article/rival-drugs-of-biogen-s-aduhelm-may-help-prove-fda-s-highly-criticized-approval/

Gross, M. (2000). Proteins that convert from α helix to β sheet: Implications for folding and disease. *Current Protein & Peptide Science, 1*(4), 339–347. https://doi.org/10.2174/1389203003381289

Halliday, M., Radford, H., Zents, K. A. M., Molloy, C., Moreno, J. A., Verity, N. C., Smith, E., Ortori, C. A., Barrett, D. A., Bushell, M., & Mallucci, G. R. (2017). Repurposed drugs targeting eIF2α-P-mediated translational repression prevent neurodegeneration in mice. *Brain*, *140*(6), 1768–1783. https://doi.org/10.1093/brain/awx074

Hunt, P. R. (2017). The *C. elegans* model in toxicity testing. *Journal of Applied Toxicology, 37*(1), 50–59. https://doi.org/10.1002/jat.3357

Jay, A. R., Krotscheck, U., Parsley, E., Benson, L., Kravitz, A., Mulligan, A., Silva, J., Mohammed, H., & Schwark, W. S. (2013). Pharmacokinetics, bioavailability, and hemodynamic effects of trazodone after intravenous and oral administration of a single

dose to dogs. *American Journal of Veterinary Research*, *74*(11), 1450–1456. https://pubmed.ncbi.nlm.nih.gov/24168312/

Krystal, A. D. (2010). Antidepressant and antipsychotic drugs. *Sleep Medicine Clinics*, *5*(4), 571–589. https://doi.org/10.1016/j.jsmc.2010.08.010

Kumar, A., Gupta, V., & Sharma, S. (2021). *Donepezil*. StatPearls Publishing. https://www.ncbi.nlm.nih.gov/books/NBK513257/

Land, M. H., Toth, M. L., MacNair, L., Vanapalli, S. A., Lefever, T. W., Peters, E. N., & Bonn-Miller, M. O. (2021). Effect of cannabidiol on the long-term toxicity and lifespan in the preclinical model *Caenorhabditis elegans*. *Cannabis Cannabinoid Research*, *6*(6), 522–527. https://doi.org/10.1089/can.2020.0103

Lebert, F., Stekke, W., Hasenbroekx, C., & Pasquier, F. (2004). Frontotemporal dementia: A randomised, controlled trial with trazodone. *Dementia and Geriatric Cognitive Disorders, 17*(4), 355–359. https://doi.org/10.1159/000077171

Lee, J. H., Jeong, S. K., Kim, B. C., Park, K. W., & Dash, A. (2015). Donepezil across the spectrum of Alzheimer's disease: Dose optimization and clinical relevance. *Acta Neurologica Scandinavica, 131*(5), 259–267. https://doi.org/10.1111/ane.12386

Lewczuk, P., Esselmann, H., Bibl, M., Beck, G., Maler, J. M., Otto, M., Kornhuber, J., & Wiltfang, J. (2004). Tau protein phosphorylated at threonine 181 in CSF as a neurochemical biomarker in Alzheimer's disease: Original data and review of the literature. *Journal of Molecular Neuroscience, 23*(1–2), 115–122. https://doi.org/10.1385/JMN:23:1-2:115

Maccarrone, M. (2017). Metabolism of the endocannabinoid anandamide: Open questions after 25 years. *Frontiers in Molecular Neuroscience*, *10*, 166. https://doi.org/10.3389/fnmol.2017.00166

Maremonti, E., Eide, D. M., Rossbach, L. M., Lind, O. C., Salbu, B., & Brede, D. A. (2020). *In vivo* assessment of reactive oxygen species production and oxidative stress effects induced by chronic exposure to gamma radiation in *Caenorhabditis elegans*. *Free Radical Biology and Medicine*, *152*, 583–596. https://doi.org/10.1016/j.freeradbiomed.2019.11.037

McClanahan, P. D., Xu, J. H., & Fang-Yen, C. (2017). Comparing *Caenorhabditis elegans* gentle and harsh touch response behavior using a multiplexed hydraulic microfluidic device. *Integrative Biology, 9*(10), 800–809. https://doi.org/10.1039/c7ib00120g

Mecha, M., Torrao, A. S., Mestre, L., Carrillo-Salinas, F. J., Mechoulam, R., & Guaza, C. (2012). Cannabidiol protects oligodendrocyte progenitor cells from inflammation-induced apoptosis by attenuating endoplasmic reticulum stress. *Cell Death & Disease*, *3*(6), e331. https://doi.org/10.1038/cddis.2012.71

Melas, P. A., Qvist, J. S., Deidda, M., Upreti, C., Wei, Y. B., Sanna, F., Fratta, W., Scherma, M., Fadda, P., Kandel, D. B., & Kandel, E. R. (2018). Cannabinoid modulation of eukaryotic initiation factors (eIF2α and eIF2B1) and behavioral cross-sensitization to cocaine in adolescent rats. *Cell Reports, 22*(11), 2909–2923. https://doi.org/10.1016/j.celrep.2018.02.065

Melzacka, M., Boksa, J., & Maj, J. (1979). l-(*m*-Chlorophenyl)piperazine: A metabolite of trazodone isolated from rat urine. *Journal of Pharmacy and Pharmacology*, *31*(1), 855–856. https://doi.org/10.1111/j.2042-7158.1979.tb13680.x

Millar, S. A., Stone, N. L., Bellman, Z. D., Yates, A. S., England, T. J., & O'Sullivan, S. E. (2019). A systematic review of cannabidiol dosing in clinical populations. *British Journal of Clinical Pharmacology, 85*(9), 1888–1900. https://doi.org/10.1111/bcp.14038

Moreno, J. A., Halliday, M., Molloy, C., Radford, H., Verity, N., Axten, J. M., Ortori, C. A., Willis, A. E., Fischer, P. M., Barrett, D. A., & Mallucci, G. R. (2013). Oral treatment targeting the unfolded protein response prevents neurodegeneration and clinical disease in prion-infected mice. *Science Translational Medicine, 5*(206), 206ra138. https://doi.org/10.1126/scitranslmed.3006767

Mori, K. (2000). Tripartite management of unfolded proteins in the endoplasmic reticulum. *Cell, 101*(5), 4510150454. https://doi.org/10.1016/s0092-8674(00)80855-7

Oakes, M. D., Law, W. J., Clark, T., Bamber, B. A., & Komuniecki, R. (2017). Cannabinoids activate monoaminergic signaling to modulate key *C. elegans* behaviors. *The Journal of Neuroscience, 37*(11), 2859–2869. https://doi.org/10.1523/JNEUROSCI.3151-16.2017

Oikonomou, G., & Shaham, S. (2011). The glia of *Caenorhabditis elegans*. *Glia*, *59*(9), 1253–1263. https://doi.org/10.1002/glia.21084

O'Sullivan, S. E. (2016). An update on PPAR activation by cannabinoids. *British Journal of Pharmacology*, *173*(12), 1899–1910. https://doi.org/10.1111/bph.13497

Park, H.-E. H., Jung, Y., & Lee, S.-J. V. (2017). Survival assays using *Caenorhabditis elegans*. *Molecules and Cells, 40*(2), 90–99. https://doi.org/10.14348/molcells.2017.0017

Radford, H., Moreno, J. A., Verity, N., Halliday, M., & Mallucci, G. R. (2015). PERK inhibition prevents tau-mediated neurodegeneration in a mouse model of frontotemporal dementia. *Acta Neuropathologica, 130*(5), 633–642. https://doi.org/10.1007/s00401-015-1487-z

Reynaud, E. (2010). Protein misfolding and degenerative diseases. *Nature Education*, *3*(9), 28. https://www.nature.com/scitable/topicpage/protein-misfolding-and-degenerative-diseases-14434929/

Ritchie, C., Smailagic, N., Noel-Storr, A. H., Ukoumunne, O., Ladds, E. C., & Martin, S. (2017). CSF tau and the CSF tau/ABeta ratio for the diagnosis of Alzheimer's disease dementia and other dementias in people with mild cognitive impairment (MCI). *Cochrane Database of Systematic Reviews, 3*, CD010803. https://doi.org/10.1002/14651858.CD010803.pub2

Ryberg, E., Larsson, N., Sjögren, S., Hjorth, S., Hermansson, N. O., Leonova, J., Elebring, T., Nilsson, K., Drmota, T., & Greasley, P. (2007). The orphan receptor GPR55 is a novel cannabinoid receptor. *British Journal of Pharmacology*, *152*(7), 1092–1101. https://doi.org/10.1038/sj.bjp.0707460

Simmons, S. O., Fan, C.-Y., & Ramabhadran, R. (2009). Cellular stress response pathway system as a sentinel ensemble in toxicological screening, *Toxicological Sciences*, *111*(2), 202–225. https://doi.org/10.1093/toxsci/kfp140

Solis, G. M., & Petrascheck, M. (2011). Measuring *Caenorhabditis elegans* life span in 96 well microtiter plates. *Journal of Visualized Experiments*, *49*, e2496. https://doi.org/10.3791/2496

Sotolongo, K., Ghiso, J., & Rostagno, A. (2020). Nrf2 activation through the PI3K/GSK-3 axis protects neuronal cells from αβ-mediated oxidative and metabolic damage. *Alzheimer's Research & Therapy, 12*(13). https://doi.org/10.1186/s13195-019-0578-9

Spina, S., Schonhaut, D. R., Boeve, B. F., Seeley, W. W., Ossenkoppele, R., O'Neil, J. P., Lazaris, A., Rosen, H. J., Boxer, A. L., Perry, D. C., Miller, B. L., Dickson, D. W., Parisi,

J. E., Jagust, W. J., Murray, M. E., & Rabinovici, G. D. (2017). Frontotemporal dementia with the V337M *MAPT* mutation: Tau-PET and pathology correlations. *Neurology, 88*(8), 758–766. https://doi.org/10.1212/WNL.0000000000003636

Strang, K. H., Golde, T. E., & Giasson, B. I. (2019). *MAPT* mutations, tauopathy, and mechanisms of neurodegeneration. *Laboratory Investigation, 99*(7), 912–928. https://doi.org/10.1038/s41374-019-0197-x

Sutton, S. (2022, March 22). Addressing the Aduhelm controversy: What is going on with Aduhelm? *The Medicine Maker*. https://themedicinemaker.com/business-regulation/addressing-the-aduhelm-controversy

Tissenbaum, H. A. (2015). Using *C. elegans* for aging research. *Invertebrate Reproduction & Development, 59*(sup1), 59–63. https://doi.org/10.1080/07924259.2014.940470

Tonnies, E., & Trushina, E. (2017). Oxidative stress, synaptic dysfunction, and Alzheimer's disease. *Journal of Alzheimer's Disease, 57*(4), 1105–1121. https://doi.org/10.3233/JAD-161088

Urban, N. D., Cavataio, J. P., Berry, Y., Vang, B., Maddali, A., Sukpraphrute, R. J., Schnell, S., & Truttmann, M. C. (2021). Explaining inter-lab variance in *C. elegans* N2 lifespan: Making a case for standardized reporting to enhance reproducibility. *Experimental Gerontology, 156*, 111622. https://doi.org/10.1016/j.exger.2021.111622

Wang, R., Mason, D. E., Choe, K. P., Lewin, A. S., Peters, E. C., & Luesch, H. (2013). *In vitro* and *in vivo* characterization of a tunable dual-reactivity probe of the Nrf2-ARE pathway. *ACS Chemical Biology*, *8*(8), 1764–1774. https://doi.org/10.1021/cb4000103

Wang, H., Zhao, Y., & Zhang, Z. (2019). Age-dependent effects of floxuridine (FUdR) on senescent pathology and mortality in the nematode *Caenorhabditis elegans*. *Biochemical*

and Biophysical Research Communications, 509(3), 694–699. https://doi.org/10.1016/j.bbrc.2018.12.161

Wilson, S. R., Strand, M. F., Krapp, A., Rise, F., Herstad, G., Malterud, K. E., & Krauss, S. (2010). Hedgehog antagonists cyclopamine and dihydroveratramine can be mistaken for each other in *Veratrum album*. *Journal of Pharmaceutical and Biomedical Analysis, 53*(3), 497–502. https://doi.org/10.1016/j.jpba.2010.05.024

Wood, H. (2017). Halting neurodegeneration — are repurposed drugs the answer? *Nature Reviews Neurology, 13*(6), 317. https://doi.org/10.1038/nrneurol.2017.71

Zanetti, O., Solerte, S. B., & Cantoni, F. (2009). Life expectancy in Alzheimer's disease (AD). *Archives of Gerontology and Geriatrics*, *49*(Supplement), 237–243. https://doi.org/10.1016/j.archger.2009.09.035

Zhang, Y., Li, H., Jin, S., Lu, Y., Peng, Y., Zhao, L., & Wang, X. (2022). Cannabidiol protects against Alzheimer's disease in *C. elegans* via ROS scavenging activity of its phenolic hydroxyl groups. *European Journal of Pharmacology*, *919,* 174829. https://doi.org/10.1016/j.ejphar.2022.174829

Zheng, W., Schafer, N. P., & Wolynes, P. G. (2013, Jan 29). Frustration in the energy landscapes of multidomain protein misfolding. *Proceedings of the National Academy of Sciences of the United States of America*, *110*(5), 1680–1685. https://doi.org/10.1073/pnas.1222130110

LIST OF ABBREVIATIONS

ACh	acetylcholine
AEA	*N*-arachidonoyl-ethanolamine, anandamide
ARE	antioxidant response element
AVA	anterior ventral process A interneuron
AVB	anterior ventral process B interneuron
AVD	anterior ventral process D interneuron
CBD	Cannabidiol
CYP	Cytochrome
DAPI	4′,6-diamidino-2-phenylindole
DOI	drug of interest
FUdR	Floxuridine
LPS	Lipopolysaccharide
PVC	posterior ventral process C interneuron
ROS	reactive oxygen species
TRA	Trazadone
UPR	unfolded protein response